Beni-Suef University Journal of Basic and Applied Sciences

RESEARCH

Open Access

Mesembryanthemum crystallinum alleviates titanium dioxide nanoparticle-induced toxicity in male rats: an ADME and in vivo study

Ibrahim A. Ibrahim[1*], Heba T. Ebeed[1,2] and Hagar E. Mohammed[3]

Abstract

Background Titanium dioxide nanoparticles (TiO_2NPs) are commonly used in industrial and consumer products, including paints, food colorants, paper, sunscreen lotions, and toothpaste. Due to growing concerns about their potential health risks, this study aimed to evaluate the bioactive constituents of the ethanolic extract of *Mesembryanthemum crystallinum* (MEE) using GC–MS and assess its protective efficacy against TiO_2NPs-induced oxidative damage.

Methods The rats were orally administered treatments for two weeks across six groups: a negative control group, a TiO_2NPs-only group (300 mg/kg b.w.), two groups receiving MEE alone (50 and 100 mg/kg b.w), and two co-treatment groups receiving TiO_2NPs with MEE at 50 and 100 mg/kg b.w, respectively. Samples of tissues and blood were collected for biochemical and histological analysis.

Results GC–MS analysis identified 32 bioactive compounds in the MEE, with major constituents including D-Pinitol, pentakis ether, and different fatty acids. TiO_2NPs were spherical (10–50 nm) with uniform size distribution. Exposure to TiO_2NPs resulted in elevated oxidative stress markers, and altered lipid profiles, as well as histopathological damage in liver, kidney, testis, and heart tissues. MEE co-treatment improved, in a dose-dependent manner, these parameters and reduced TiO_2NPs accumulation in liver and kidney tissues. Moreover, in silico pharmacokinetic and toxicity predictions revealed favorable LD50 values (1500–2280 mg/kg) and excellent bioavailability for key compounds.

Conclusion *M. crystallinum* extract demonstrates a strong antioxidant and chelating properties, making it a promising nutraceutical candidate for mitigating TiO_2NPs-induced toxicity and enhancing clearance of accumulated nanoparticles from vital organs.

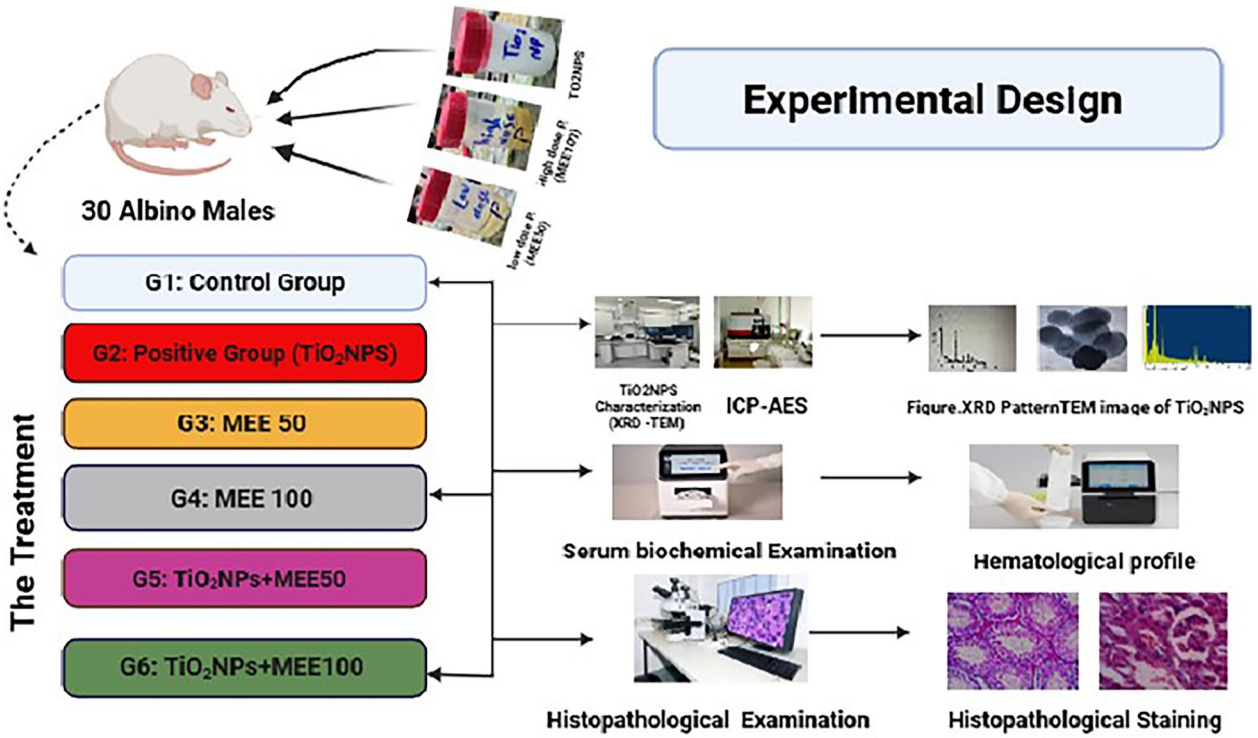
Keywords ADMET, *Mesembryanthemum crystallinum* L., Nanoparticles, Oxidative stress, Titanium dioxide

*Correspondence:
Ibrahim A. Ibrahim
ibrahimashour175@gmail.com
Full list of author information is available at the end of the article

Springer Open

© The Author(s) 2025. **Open Access** This article is licensed under a Creative Commons Attribution 4.0 International License, which permits use, sharing, adaptation, distribution and reproduction in any medium or format, as long as you give appropriate credit to the original author(s) and the source, provide a link to the Creative Commons licence, and indicate if changes were made. The images or other third party material in this article are included in the article's Creative Commons licence, unless indicated otherwise in a credit line to the material. If material is not included in the article's Creative Commons licence and your intended use is not permitted by statutory regulation or exceeds the permitted use, you will need to obtain permission directly from the copyright holder. To view a copy of this licence, visit http://creativecommons.org/licenses/by/4.0/.

Graphical abstract



1 Introduction

Recently, nanoscience has experienced rapid growth, driven by the expanding field of nanotechnology and its diverse applications [1]; it is also called as the industrial revolution of the twenty-first century. Extensive research, development, and manufacturing methods have been used worldwide to create better and safer nanomaterials for various applications [2]. The design, fabrication, and management of materials (1–100 nm) are made possible by nanotechnology, which is the manipulation of materials at an incredibly small scale [3]. Numerous industries, including electronics, manufacturing, healthcare, and agriculture, cosmetics, and pharmaceutical industries use nanoparticles (NPs) [4]. They are used as additives in a variety of products, including food, paints, ceramics, paper packaging, drug delivery systems, biosensors, and cancer treatments. NPs are present in about 1000 products that are presently available [5]. The molecules increase exponentially as particle size decreases, giving NPs an increase from surface area-to-volume ratio than with bulk materials. This affects physical characteristics by increasing surface reactivity. Nanoproducts are commonly used due to their small size and reactive surface, which has sparked worries about hazards to human health and the environment. The reduced size of NPs also alters their biokinetics, enabling them to spread more easily throughout the body [6]. Many studies have reviewed how NPs can access the cell nucleus and have shown their genotoxic potential. Interference with DNA repair enzymes and DNA-related proteins could be the cause of this [7].

Titanium dioxide (TiO_2) is one of the major utilized materials among the top five NPs produced. Some of the industries that use it in its nanoform include chemical fibers, toothpaste, pharmaceuticals, catalysts, metallurgy, environmental cleanup of air, soil, and water [8]. Due to growing use of TiO_2NPs in industry fields and nanotechnology products, human exposure—intentional or not—is increasingly concerning [8]. Despite their extensive use, studies have shown that TiO_2NPs can cause apoptosis in the heart, spleen, liver, lungs, gastrointestinal system, and kidney upon exposure [9]. It has been demonstrated that TiO_2NPs change heart rate, damage small intestine, and produce neurotoxicity in the human brain [10]. In addition, multiple animal models have demonstrated that TiO_2NPs cause genotoxicity in bone marrow cells [11], hepatotoxicity, kidney damage [12], splenitis

[13], and impaired immune response [14], leading to oxidative stress, inflammation, and apoptosis [15].

Medicinal plants have played essential part in disease treatment since ancient times and are still a valuable source of therapeutic agents. Many of these plants have been investigated in vitro for their potential medical benefits. Studies on pharmacology have emphasized the significance of medicinal plants as possible sources of bioactive substances [17]. Extracts from certain plants have been evaluated using modern medicinal systems and have been found to positively influence the activities of several regulatory enzymes [19]. Medicinal herbs are known to exhibit their antioxidative properties by altering antioxidant defense mechanisms and scavenging reactive oxygen species like Indica which has antioxidant, neuroprotective and anti-inflammatory properties [20]. There are several medicinal plants that are used in decreasing TiO_2NPs toxicity such as *Cinnamomum cassia*, *Moringa oleifera* leaves [21], *Moringa oleifera* seed, Milk Thistle seeds [22]. *Mesembryanthemum crystallinum L.* (*M. crystallinum*) is a member of the Aizoaceae family. Numerous kinds of chemicals are known to exist in the Aizoaceae family. *M. crystallinum*, also known as the ice plant, has been traditionally used as a medicinal plant. This plant's leaves include catechin, ferulic acid, catechol tannins, and flavonoids (rutin, neo-hesperidin, hyperoxide, phenolics [23], carotenoids, saponins, tannins, alkaloids, and polyphenols [24] The epidermal bladder cells on the stem and leaves resemble ice crystals, hence the name "ice plant." These bladder cells contain inositol, beta-carotene, and various minerals [25], as well as myo-inositol, which lowers triglyceride levels, and pinitol, which helps lower blood sugar levels, making the plant advantageous for diabetic people. Additionally, *M. crystallinum* has shown antibacterial [26], antioxidant [27], anti-inflammatory [25], and memory-improving effects [28]. The plant has a fresh, salty, lemony flavor and an excellent nutritional profile [29]. Thus, the purpose of this work is to address a significant research gap by examining the ability of *M. crystallinum* to mitigate TiO_2NPs toxicity, specially focusing on its chelating properties.

2 Materials and methods

2.1 Materials

The source of titanium tetra-isopropoxide (TTIP) was Sigma-Aldrich (St. Louis, MO, USA). Kits for liver and kidney functions, along with lipid profiles and lipoproteins assays, were supplied by Randox Co. (Antrim, UK). Creatine kinase (ab155901) and lactate dehydrogenase enzyme kits were acquired from the Egyptian Company of Biotechnology (Egypt) and Abcam respecrively. Antioxidant enzyme kits were provided by Eagle Diagnostics (Dallas, TX, USA). Sigma (St. Louis, MO, USA) also provided the trypan blue dye, MTT, and dimethyl sulfoxide (DMSO). Cell culture reagents including fetal bovine serum, DMEM, HEPES buffer solution, L-glutamine, gentamycin, and 0.25% trypsin–EDTA were purchased from Lonza (Belgium).

2.2 Preparation of plant extract

During May 2023, *M. crystallinum* plant was collected and taxonomically authenticated, where voucher specimens were kept in the Herbarium under accession number A4483. Fresh aerial parts of *M. crystallinum* (Fig. 1a) were rinsed thoroughly with running tap water, blotted dry with a clean cloth, and left in the dark for seven days.

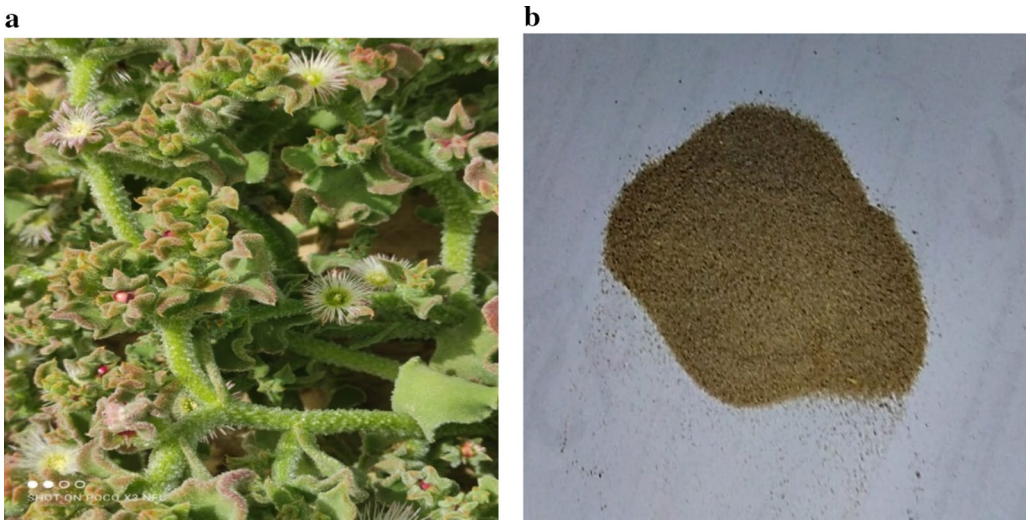


Fig. 1 *Mesembryanthemum crystallinum* fresh form (Fig. 1a) and extracted form (Fig. 1b)

Then, plant material was oven-dried for two hours at 60 °C and crushed into a fine powder [26]. Microwave-assisted extraction technique was employed using aqueous ethanol (Fig. 1b), and the resulting extract was stored at 4C° until further use [30].

2.3 Phytochemical analysis of *M. crystallinum*

2.3.1 Total phenolic content (TPC)

By using a colorimetric technique and the Folin–Ciocalteu reagent, the extracts' total phenolic content was ascertained. Following the incubation period, a reagent blank was used to assess the absorbance at 765 nm. Gallic acid equivalent (GAE) mg/g was used to express the overall phenolic content [31].

2.3.2 Total flavonoid content (TFC)

The flavonoids compounds were assessed using a modified AlCl3 colorimetric method. After incubation, the absorbance was measured at 510 nm, and the results were expressed as micrograms of quercetin equivalent (Qu) per gram of dry extract [31].

2.3.3 Determination of tannins

Tannic acid was used as the reference standard to determine the tannin concentration. The absorbance was measured at 500 nm according to Broadhurst and Jones [32] method.

2.3.4 Total saponins content (TSC)

2.3.4.1 Preparation of the standard curve To determine the total saponin content (TSC), one gram of powdered sample in a conical flask was mixed with 30 mL of ethanol according to technologies [33]. A Biosystem 310 spectrophotometer was used to measure absorption at 560 nm and calibrated with the blank. The standard curve was generated from absorbance values to quantify total saponin content. TSC was calculated according to the following equation:

TSC = (weight of saponin in the extract (mg)) / ((weight of powder (g)) x (1—(moisture %/100)).

Results were expressed as mg of aescin equivalent per g of dry powder (mg AE/g).

2.3.5 Determination of total carbohydrates

About 100 mg of plant material was weighed and placed in a 10 mL boiling tube containing distilled water and then incubated for three hours in a water bath. After cooling, sodium carbonate was added to neutralize the solution and stop the effervescence. The volume was adjusted to 100 mL with distilled water and centrifuged. The resulting supernatant was collected and used for further analysis. Glucose was used as the standard, and absorbance was measured at 490 nm using a Biosystem 310 Plus spectrophotometer, following the method described by Roberts and Elias [34].

2.3.6 Total antioxidant capacity (TAC)

Antioxidant activity was assessed using the method described by Prieto et al. method [35], where absorbance measured at 695 nm was determined. TAC was quantified and expressed as milligrams of gallic acid equivalents per gram of extract (mg GAE) [36].

2.3.7 Evaluation of cytotoxicity against BHK-21 cell line

The cells were cultured in DMEM enriched with additional nutrients at 37 °C with 5% CO_2 incubator. To conduct cytotoxicity, 1×10^4 cells were planted in 96-well plates and treated with serial dilutions of the test compound for 24 h. Cell viability was evaluated using the MTT test, with absorbance measured at 590 nm. GraphPad Prism was used to create dose–response curves in order to calculate the cytotoxic concentration (CC50) [37].

2.4 Identification of volatile hydrocarbon compound by gas chromatography-mass spectrometry (GC–MS)

Volatile hydrocarbon compounds were identified by GC–MS according to Nekeety et al. [38]. Hydrocarbons (C7–C20, Aldrich Co.) were references to calculate the isolated volatile components [39].

2.5 Preparation of TiO_2NPs

The physical grinding approach was used to reduce the particle size TiO_2 powder. After grinding, the fine powder was separated and stored in plastic bag at room temperature until further use [40].

2.6 Characterization of TiO_2NPs

2.6.1 TiO_2NPs characterization by XRD-frication

The generated TiO_2NPs sample was analyzed by X-ray diffraction (XRD) utilizing Cu-Kα X-rays with a wavelength (λ) of 1.5406 Å and a Bruker diffractometer. The results confirmed the size of the nanoparticles in the TiO_2 powder [40].

2.6.2 Characterization of TiO_2NPs by transmission electron microscopy (TEM)

At the Desert Research Center in El Matareya, Cairo, Egypt, TiO_2NPs were characterized. For TEM analysis, copper grids were coated with a droplet of the TiO_2NPs suspension, air-dried, and then examined under a high-resolution TEM to assess particle morphology and size distribution.

2.7 Experimental animals

Two-month-old male adult albino rats, weighing between 150 and 200 g, were acquired from Mansoura University's breeding center, Mansoura, Egypt. All experimental treatment adhered to the National Institutes of Health's guidelines for the care and use of laboratory animals (NIH Publication No. 8023, revised 1978) and were approved by the Animal Care and Use Committee of the Faculty of Science, Arish university (approval no. ARU/SF.12#), ensuring humane treatment throughout the study.

2.8 Study design

After a one-week adaptation period, animals were split into six groups randomly (5 animals per group), as outlined in Scheme 2. TiO_2NPs were administered orally at a dose of 300 mg/kg b.w/day, following the protocol of Orazizadeh et al. [41]. Furthermore, *M. crystallinum* ethanolic extract (MEE) was given at two concentrations: low concentration of 50 mg/kg b.w/day/PO based on Lee et al. [28] and a high concentration 100 mg/kg b.w/day/PO, achieved by doubling the low concentration of MEE. The animals had free access to water and starved overnight after the final treatment.

Throughout the 14-day experimental period, body weight was recorded at the beginning and end of the study for each group. On day 15, blood samples were collected under isoflurane anesthesia. For hematological examination, samples were placed into EDTA-coated tubes, while separate plain tubes were used for serum collection. After clotting, serum was separated by refrigerated centrifugation and kept at − 80 °C until further analysis.

After dissection, selected organs—including the liver, heart, stomach, testes, and kidneys—were immediately removed, rinsed in saline, and weighed. Relative organ weight was calculated by dividing the absolute organ weight by the final body weight and multiplying by 100.

Biochemical analysis—including liver and kidney function, lipid profile, and cardiac function (LDH and CK), was performed using spectrophotometer following the manufacturer's instruction. After blood collection, samples of liver and kidneys were taken out, weighed, and homogenized in phosphate buffer (pH 7.4) [42]. Antioxidant enzyme activities and GSH content were measured in both serum and tissue supernatants using spectrophotometric methods. For histological analysis, liver, kidney, heart, as well as testicular tissues were preserved in formalin, cleared in xylene, and embedded in paraffin. Sections of 5 µm thickness were prepared and stained with hematoxylin and eosin (H&E) following the protocol described by Bancroft & Gamble [44] and examined using an Olympus BX 52 microscope (Fig. 2).

2.9 Inductively coupled plasma mass spectroscopy (ICP-MS)

For digestion, each tissue sample was oven-dried and mixed with 200 mg of NH4Cl, 2 mL of 96% H2SO4, and 2 mL of 65% HNO_3. The digestion process was conducted using a microwave assisted program with sequential power settings: 500W for five minutes, 400W for five minutes, 650W for five minutes, and 250W for five minutes. After complete cooling, the digested solutions were transferred to 10 mL graduated flasks and diluted with distilled water. After being diluted five times, the solutions were kept at 5 °C until they could be analyzed. Before examining the samples, the spectrometer was recalibrated using a freshly prepared calibration curve. Every sample was measured in triplicates to ensure data accuracy and repeatability.

2.10 In Silico absorption, distribution, metabolism, excretion, and toxicity (ADMET) analysis of *M. crystallinum* compounds

The Swiss ADME server (http://www.swissadme.ch/index.php) was used to evaluate the ADMET characteristics of the phytochemicals identified in MEE extract. The compounds' physicochemical properties, lipophilicity, water solubility, pharmacokinetics, drug-likeness, and medicinal chemistry aspects are provided on this platform. Additionally, the web servers StopTox (https://stoptox.mml.unc.edu/) [45] and ProTox-II (https://tox-new.charite.de/protox_II/) [46] were used to evaluate the toxicity characteristics of the discovered phytochemicals. While StopTox offered predictions for cardiotoxicity (hERG liability), ProTox-II predicted the toxicity class and LD50 (lethal dose 50%) of the listed phytochemicals.

2.11 Statistical analysis

Software Graph Pad Prism 8.0.1 (San Diego, CA, USA) was used to analyze the data. The data are presented as mean ± SEM for each group ($n=5$). Statistical significance between groups was conducted using one-way analysis of variance (ANOVA) followed by Tukey's multiple comparisons test. A p value < 0.05 was considered statistically significant. Significance levels relative to control group were indicated as follows: $^{*}P<0.05$, $^{**}P<0.01$, $^{***}P<0.001$, and $^{****}P<0.0001$. The group comparisons for TiO_2NPs were $^{\#}P<0.05$, $^{\#\#}P<0.01$, $^{\#\#\#}P<0.001$, and $^{\#\#\#\#}P<0.0001$.

3 Results

3.1 Phytochemical composition of *M. crystallinum*

Table 1 shows the quantified levels of total phenolics, flavonoids, tannins, saponins, and carbohydrates in the extract. Among these, total phenolics exhibited the highest concentration (41.86 ± 2.26 mg/g), indicating strong

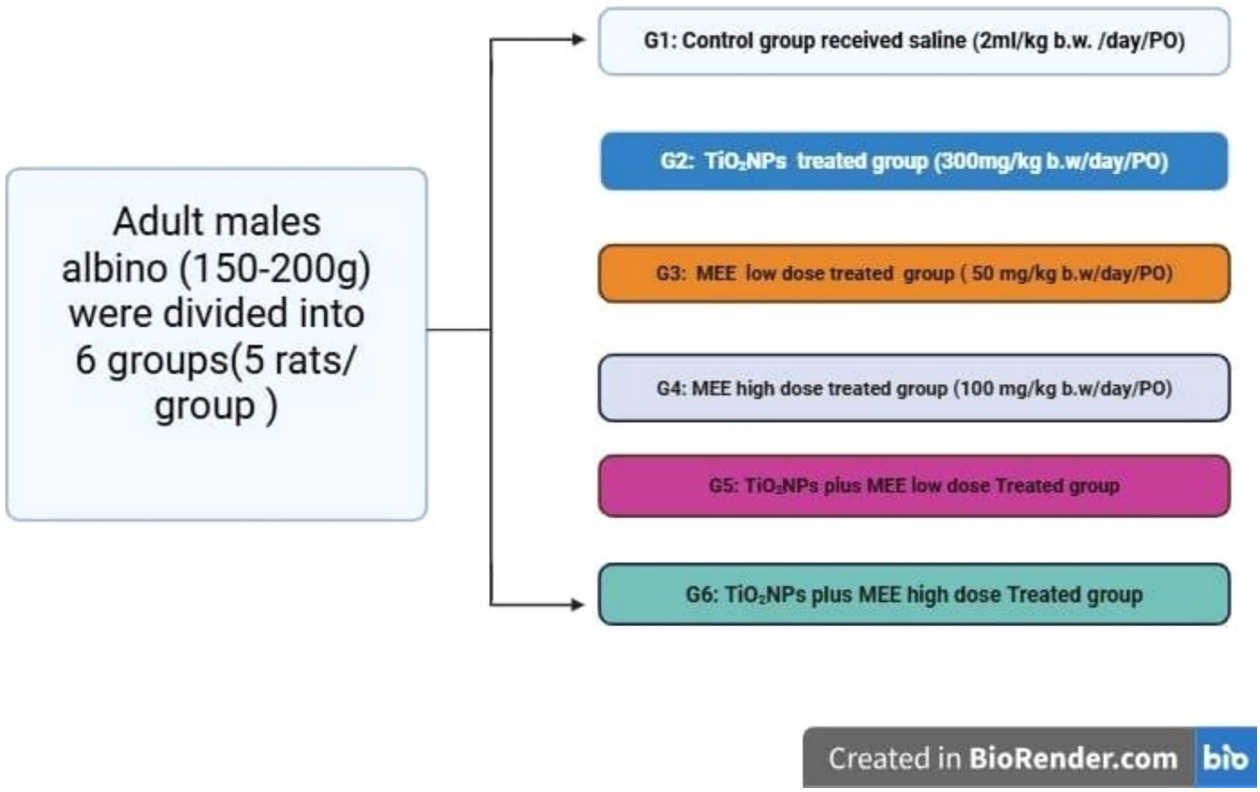


Fig. 2 Created by BioRender.Com, showing treatment schedule

Table 1 Phytochemicals compounds and total carbohydrates of *M. crystallinum*. The mean ± SD of three separate calculations at $p < 0.05$ was used to express the values

M. crystallinum	(mg/g)
Total phenolics	41.86 ± 2.26
Total flavonoids	30.02 ± 0.59
Total tannins	12.61 ± 0.84
Total saponins	28.66 ± 1.20
Total carbohydrates	580.33 ± 11.05

Table 2 Antioxidant activity of *M. crystallinum*. The mean ± SD of three separate calculations at $p < 0.05$ was used to express the values

Sample	TAC (mg GAE/g)
MEE	23.79 ± 1.03
Ascorbic acid (positive control)	76.12 ± 3.24

antioxidant potential. On the other hand, total tannins showed the lowest content (12.61 ± 0.84 mg/g). Notably, total carbohydrates were present at a significantly higher level (580.33 ± 11.05 mg/g), reflecting the extract's rich nutritional composition.

3.2 Antioxidant activity of *M. crystallinum*

The antioxidant activity of *M. crystallinum* extract and ascorbic acid, expressed as milligrams of gallic acid equivalents per gram (mg GAE/g), is presented in Table 2. The extract exhibited an antioxidant capacity of 23.79 ± 1.03 mg GAE/g, while ascorbic acid showed higher activity at 76.12 ± 3.24 mg GAE/g.

3.3 Evaluation of cytotoxicity of *M. crystallinum* extract against BHK-21 cell line

Table 3 shows the cytotoxic effect *M. crystallinum* extract on the BHK-21 cell line across a range of concentrations (0–1000 µg/ml). The highest inhibition was observed at 1000 µg/ml, reaching 88.93 ± 1.51%; meanwhile, the lowest inhibition occurred at 15.6 µg/ml (0.43 ± 0.15%). No inhibitory activity was detected at concentrations of 0, 2, 3.9, and 7.8 µg/ml (inhibition = 0%). The 50% cell cytotoxic concentration (CC50) was calculated to be 281.32 ± 8.94 µg/ml, indicating lowest cytotoxic potential of the extract.

Table 3 Effect of *M. crystallinum* on cytotoxicity against BHK-21 cell line

M. crystallinum conc. (µg/ml)	Viability %	Inhibitory %
1000	11.07	88.93 ± 1.51
500	30.94	69.06 ± 1.82
250	52.73	47.27 ± 2.35
125	74.15	25.85 ± 1.83
62.5	88.46	11.54 ± 0.82
31.25	96.79	3.21 ± 0.53
15.6	99.57	0.43 ± 0.15
7.8	100	0
3.9	100	0
2	100	0
0	100	0

3.4 GC–MS analysis of *M. crystallinum*

GC–MS analysis identified 32 phytochemical compounds in *M. crystallinum* extract (Table 4 and Fig. S1). These compounds were classified as ester, ether, glycoside, silane, heterocyclic compound. Ester was the most abundant (55.99%), followed by ether (32.68%), glycoside (6.5819%), silane (2.3%), heterocyclic compound (1.8267%), and epoxide (0.6406%) (Fig. S2).

3.5 Characterization of TiO_2NPs by XRD diffraction and transmission electron microscope

The prepared sample's phase was examined using the X-ray diffraction (XRD) technique. Results revealed that TiO_2 NPs peaks were obtained at ($2\theta = 24.8°$, 37.2°, 47.7°, 53.6°, 55.04°, and 62.2°) with the corresponding reflection planes of (101), (004), (200), (211), (220), and (118). The XRD (X-ray diffraction) patterns of TiO_2NPs revealed a prominent peak at $2\theta = 24.8°$, which confirms the presence of the anatase phase of TiO_2. This peak is characteristic of the anatase structure, a common crystalline form of TiO_2. Additional strong diffraction peaks at 24.8° and 47.7° further support the anatase structure. As the particle size increased, the intensity of the XRD peaks also increased, suggesting enhanced crystallinity and structural ordering. The broadness of the peaks indicates nanoscale crystallite dimensions, consistent with typical nanoparticle features (Fig. S3). TEM images (Fig. S4a and S4b) showed spherical shape particles with uniform size distribution. TiO_2 nanoparticles are aggregated together and are composed of primary particles with diameters between 10 and 50 nm. This result is confirmed by the crystallite size. The characterization of TiO_2NPs aggregates using TEM provides valuable insights into their size and shape. The morphometric analysis of randomly selected fields ($n \geq 100$ aggregates) was found to be 34 ± 9 nm. This result is in line with the expected range for nanoparticles, relatively indicated low standard deviation.

3.6 The impact of MEE on final body and relative organs weight (RW) in rats treated with TiO_2NPs

In Vivo findings revealed a significant reduction in body weight among rats exposed to TiO_2NPs and MEE compared to control group (Fig. 3). Notably, the co-treatment MEE did not produce any significant effect on body weight. Regarding organ weights, the TiO_2NPs-treated group showed no significant changes in relative organ weights, with exception of a pronounced decrease in the relative weight of the testes when compared to the control group (Table 5).

The values were displayed as mean ± SE (n = 5). Statistical analysis was performed using one-way ANOVA followed by Tukey's test. Symbols indicate significant differences: $^{*}P < 0.05$ versus control group; $^{\#}P < 0.05$ versus TiO_2NPs-treated group.

The values were displayed as mean ± SE (n = 5). Statistical analysis was performed using one-way ANOVA followed by Tukey's test. Symbols indicate significant differences: $^{*}P < 0.05$ versus control group; $^{\#}P < 0.05$ versus TiO_2NPs-treated group.

3.7 The impact of MEE on hematological parameters in rats treated with TiO_2NPs

Hematological indices did not show significantly significant alterations across treatment groups (Table 6). However, a slight elevation in HB levels was noted in both MEE100 and TiO_2NPs + MEE100 treated groups. Additionally, the TiO_2NPs-treated group exhibited a significant increase in lymphocyte count compared to the control group, suggesting a potential immunomodulatory response.

The values were displayed as mean ± SE (n = 5). Statistical analysis was performed using one-way ANOVA followed by Tukey's test. Symbols indicate significant differences: $^{*}P < 0.05$ versus control group; $^{\#}P < 0.05$ versus TiO_2NPs-treated group.

3.8 MEE's influence on serum biochemical markers in rats was given TiO_2NPs treatment

Biochemical analysis of liver, kidney, and cardiac function markers (Table 7) revealed that with the exception of γ-GT activity, which remain unchanged across groups, and TP and ALB, which displayed non-significant declines, all other parameters were elevated in the TiO_2NPs-treated group. CK activity was significantly increased (twofold) compared to the control group ($p < 0.05$), indicating potential cytotoxic effects. Although

Table 4 The phytochemical components of *M. crystallinum* identified by GC–MS

No	RT	Compound Name	Molecular weight (g/mol.)	Molecular formula	Area %
Glycoside 1 10.9712		α-D-Galactopyranoside, methyl 2,3-bis-O-(trimethylsilyl)-, cyclic phenylboronate	746.42	$C_{19}H_{33}BO_6Si$	6.5819
Ether 2 11.1314		1,5-Anhydrohexitol, 4TMS derivative	287.35	$C_{18}H_{44}O_5Si_4$	5.6061
3	11.2344	D-Pinitol, pentakis(trimethylsilyl) ether	412.73	$C_{24}H_{47}O_4Si_5$	20.5217
4	14.7076	16-Hydroxydehydroandrosterone, 2TMS derivative	435.65	$C_21H_{30}O_3$	1.2547
5	15.1539	(Methoxymethyl) trimethylsilane	104.22	$(CH3)_3SiOCH_3$	1.3193
6	15.0795	2-Mono-isobutyrin, 2TMS derivative	144.21	$C_5H_{10}O_2$	0.7114
7	15.2169	2-Mono-isobutyrin, 2TMS derivative	56.08	$C_7H_{14}O_2$	2.3491
8	15.3828	2-Butene-1,4-diol, (E)-, 2TMS derivative	264.36	$C_4H_8O_2$	0.3993
9	15.7719	2-Butene-1,4-diol, (E)-, 2TMS derivative	284.40	$C_4H_8O_2$	0.3215
10	16.0981	1-Trimethylsilyloxy-n-octene	204.32	$C_{11}H_{24}Osi$	0.0902
11	18.2953	1,5-cis,8-cis-Undecatriene-3,7-diol bis(trimethylsilyl)ether	276.23	$C_{23}H_{48}O_5Si_2$	0.1109
Esters and fatty acids 12 12.3044		Palmitic Acid, TMS derivative	256.42	C19H40O2Si	7.3406
13	13.1169	Linoleic acid, TMS	280.45	$C_{18}H_{32}O_2$	33.1259
14	13.1913	Stearic acid, TMS derivative	378.61	$C_{21}H_{44}O_2Si$	8.7317
15	14.6103	17-Octadecynoic acid, TMS derivative	342.45	$C_{39}H_{67}FO_2Si$	0.5857
16	14.6847	2-Oxovaleric acid, TBDMS derivative	152.22	$C_6H_{10}O_3$	1.0032
17	14.925	17-Octadecynoic acid, TMS derivative	246.46	$C_{18}H_{34}O_2$	0.7234
18	15.0566	15-Tetracosenoic acid, (Z)-, TMS derivative	341.35	$C_{19}H_{36}O_2$	1.2326
19	15.4171	13-Octadecenoic acid, (Z)-, TMS derivative	294.39	$C_{18}H_{34}O_2$	1.506
20	15.5831	2-Butoxyethoxy) acetic Acid, TMS derivative	204.27	$C_8H_{16}O_4$	0.3672
21	15.646	13-Octadecenoic acid, (E)-, TMS derivative	296.39	$C_{18}H_{34}O_2$	0.3877
22	15.7891	13-Octadecenoic acid, (E)-, TMS derivative	414.55	$C_{18}H_{34}O_2$	0.5643
23	15.9264	Linoleic acid, trimethylsilyl ester	339.54	$C_{22}H_{38}O_2Si$	0.2666
24	18.6386	4-Piperidinecarboxylic acid, 4-phenyl-1-(trimethylsilyl)-, trimethylsilyl ester	343.52	$C_{18}H_{23}NO_3Si_2$	0.1619
Epoxide 25 15.892		1,2–15,16-Diepoxyhexadecane	272.38	$C_{16}H_{30}O_2$	0.3179
26 16.0237		1,2–15,16-Diepoxyhexadecane	286.41	$C_{16}H_{30}O_2$	0.3227
Heterocyclic compound 27 16.9735		1,2-Benzisothiazole, 3-(hexahydro-1H-azepin-1-yl)-, 1,1-dioxide	261.31	$C_{13}H_{14}N_2O_3S$	1.8267
Silane 28 17.1337		Silane, [1,1-dimethyl-2-propenyl) oxy]dimethyl-	48.04	$C_8H_{18}Osi$	0.5983
29	18.3639	Silane, [1,1-dimethyl-2-propenyl) oxy]dimethyl-	130.263	$C_6H_{14}SiO$	0.533
30	18.4269	Silane, [1,1-dimethyl-2-propenyl) oxy]dimethyl-	130.263	$C_8H_{18}OS$	0.7643
31	18.4841	Silane, [1,1-dimethyl-2-propenyl) oxy] dimethyl-	130.263	$C_8H_{18}Osi$	0.232
32	18.5013	Silane, [(1,1-dimethyl-2-propenyl) oxy]dimethyl-	130.263	$C_8H_{18}Osi$	0.1514

LDH levels were elevated, the increase did not reach statistical difference. Co-treatment with MEE at both doses resulted in marked reductions in ALT, AST, urea, uric acid, and creatinine levels, suggesting a protective effect. However, CK levels remained unaffected by MEE co-treatment. Notably, the high-dose MEE group (MEE100) successfully normalized uric acid, AST, and creatinine levels, although ALT levels remained elevated relative to the control.

The values were displayed as mean ± SE ($n = 5$). Statistical analysis was performed using one-way ANOVA followed by Tukey's test. Symbols indicate significant differences: $^{*}P < 0.05$ versus control group; $^{\#}P < 0.05$ versus TiO_2NPs-treated group.

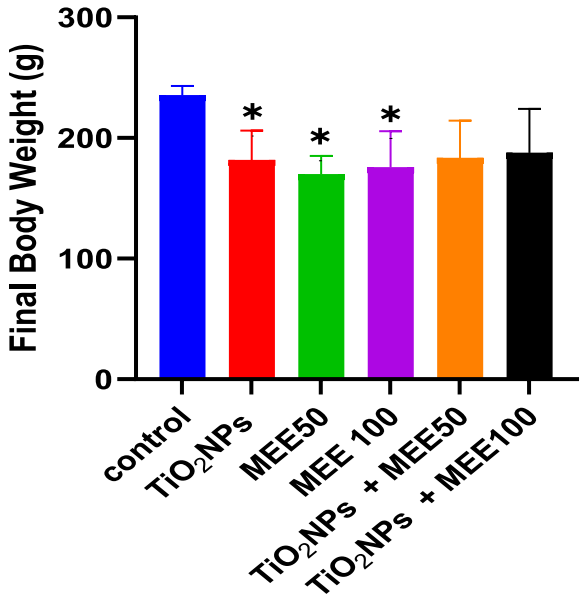


Fig. 3 Body weight of rats administered TiO_2NPs for 14 days and daily MEE

3.9 MEE's influence of MEE on the lipid profile in rats given TiO_2NPs

Table 8 summarizes the impact of various treatments on lipids. Administration of TiO_2NPs led to a significant elevation in CHO and total lipid levels compared to the control group, while TG, LDL, and HDL remained unaffected. Co-treatment with MEE at both tested dosages resulted in a dose-dependent decrease in these parameters levels, indicating a potential lipid-lowering effect on the extract.

The values were displayed as mean ± SE (n = 5). Statistical analysis was performed using one-way ANOVA followed by Tukey's test. Symbols indicate significant differences: $^{*}P < 0.05$ versus control group; $^{\#}P < 0.05$ versus TiO_2NPs-treated group.

3.10 Effect of MEE on oxidative stress markers in rats treated with TiO_2NPs

In the present investigation, exposure to TiO_2NPs results in a significant increase in MDA levels in serum, liver, and kidney tissues (Figs. 4, 5A & 6A), indicating elevated lipid peroxidation and oxidative stress. Despite a drop in serum antioxidant levels, CAT activity in hepatic and renal tissues remained unchanged. Administration of MEE alone at both tested doses showed no discernible changes in oxidative markers, except for a notable rise in SOD activity at the higher dose. Co-treatment with TiO_2NPs and MEE led to marked improvements in oxidative markers, especially in MDA, GPx, SOD, and GSH

Table 5 Effect of MEE on organ RW in rats treated with TiO_2NPs

Parameters	Control	TiO_2NPs	MEE50	MEE 100	TiO_2NPs + MEE50	TiO_2NPs + MEE100
Liver RW (%)	3.032 ± 0.1690	2.62 ± 0.38	3.74 ± 0.21	3.33 ± 0.17	3.62 ± 0.31	3.31 ± 0.11
Heart RW (%)	0.36 ± 0.02	0.39 ± 0.01	0.41 ± 0.01	0.38 ± 0.01	0.38 ± 0.02	0.43 ± 0.03
R. kidney RW (%)	0.35 ± 0.02	0.34 ± 0.02	0.38 ± 0.01	0.38 ± 0.01	0.42 ± 0.02	0.43 ± 0.03$^{\#}$
L. kidney RW (%)	0.38 ± 0.02	0.38 ± 0.02	0.41 ± 0.04	0.41 ± 0.01	0.41 ± 0.01	0.43 ± 0.02
R. Testis RW (%)	0.54 ± 0.03	0.65 ± 0.03*	0.57 ± 0.03	0.62 ± 0.04	0.61 ± 0.02	0.63 ± 0.02
L. Testis RW (%)	0.55 ± 0.03	0.69 ± 0.03*	0.58 ± 0.03	0.61 ± 0.03	0.58 ± 0.01	0.63 ± 0.03

Table 6 Impact of MEE on hematological parameters in rats treated with TiO_2NPs

Parameters	Control	TiO_2NPs	MEE50	MEE 100	TiO_2NPs + MEE50	TiO_2NPs + MEE100
RBCs ($\times 10^6$/mm^3)	5.067 ± 0.04	4.57 ± 0.29	5.29 ± 0.22	5.30 ± 0.70	3.29 ± 0.29	4.92 ± 0.29
HB (g/dL)	8.73 ± 0.32	7.97 ± 0.15	9.18 ± 0.25	13.27 ± 0.32***	8.43 ± 0.58	11.21 ± 0.23$^{\#\#\#}$
HCT (%)	35.43 ± 0.57	28.40 ± 3.28	36.08 ± 1.58	30.73 ± 3.92	26.63 ± 2.11	33.07 ± 1.24
MCV (FL)	72.80 ± 2.82	61.77 ± 4.01	67.65 ± 3.66	57.73 ± 0.17*	61.40 ± 3.06	56.10 ± 1.16
MCH (pg)	22.43 ± 2.52	17.53 ± 0.98	22.09 ± 2.41	27.47 ± 3.09	35.87 ± 1.98	24.33 ± 1.01$^{\#\#\#}$
MCHC (g/dl)	29.27 ± 1.786	28.73 ± 3.24	31.82 ± 3.45	53.43 ± 8.08	47.80 ± 9.61	43.10 ± 1.05
WBCs ($\times 10^3$/mm^3)	5.83 ± 1.03	12.43 ± 1.13	6.54 ± 1.18	10.27 ± 3.35	12.60 ± 1.24	5.67 ± 0.43
LYM (%)	34.01 ± 0.67	42.20 ± 1.36**	34.12 ± 1.04	34.40 ± 0.91	40.83 ± 1.73	36.62 ± 1.34
NEUT (%)	50.14 ± 1.48	48.47 ± 1.57	49.65 ± 0.23	52.10 ± 1.35	51.50 ± 1.31	56.51 ± 0.87$^{\#\#}$
PLT ($\times 10^3$/mm^3)	294.0 ± 15.37	220.3 ± 9.94	293.3 ± 9.35	229.7 ± 36.99	226.3 ± 13.13	322.3 ± 31.86

Table 7 Effect of MEE on serum biochemical markers in rats given TiO_2NPs treatment

Parameters	Control	TiO_2NPs	MEE50	MEE 100	TiO_2NPs + MEE50	TiO_2NPs + MEE100
TP (g/dL)	5.99 ± 0.21	5.18 ± 0.31	6.30 ± 0.16	6.50 ± 0.12	5.73 ± 0.6	6.235 ± 0.18#
ALB (g/dL)	3.13 ± 0.27	2.59 ± 0.36	3.71 ± 0.28	3.59 ± 0.09	3.23 ± 0.23	3.56 ± 0.14
ALT(IU/L)	58.22 ± 5.62	85.87 ± 3.36***	52.47 ± 3.43	50.70 ± 3.58	69.91 ± 2.26	64.11 ± 2.91##
AST(IU/L)	28.43 ± 1.47	40.72 ± 1.59**	27.14 ± 1.94	24.04 ± 2.08	30.65 ± 1.78##	28.71 ± 1.44##
γ-GT (IU/L)	32.69 ± 0.55	35.84 ± 1.52	31.18 ± 1.23	29.80 ± 1.55	31.99 ± 31.19	31.19 ± 1.03
Urea (g/dL)	26.25 ± 2.93	48.25 ± 5.25***	28.00 ± 2.48	23.75 ± 1.89	35.25 ± 2.02	32.00 ± 1.68#
CREA(g/dL)	1.03 ± 0.12	2.05 ± 0.16***	0.84 ± 0.03	0.75 ± 0.04	1.07 ± 0.09###	1.06 ± 0.09###
Uric acid (g/dL)	3.65 ± 0.20	8.09 ± 0.67***	2.81 ± 0.26	2.05 ± 0.25	3.79 ± 0.27###	3.45 ± 0.29###
LDH (U/ml)	28.48 ± 2.54	37.43 ± 1.87	26.85 ± 2.21	26.25 ± 1.30	33.95 ± 2.47	30.98 ± 2.12
CK (pg/mL)	126.0 ± 6.72	240.0 ± 28.58***	136.5 ± 5.52	133.3 ± 9.810	207.0 ± 3.11	181.3 ± 13.03

Table 8 Effect of MEE on lipid profile in rats TiO_2NPs

Parameters	Control	TiO_2NPs	MEE50	MEE 100	TiO_2NPs + MEE50	TiO_2NPs + MEE100
CHO (mg/dL)	104.30 ± 6.01	143.80 ± 5.79***	108.0 ± 5.72	90.50 ± 2.63	115.50 ± 2.59##	105.50 ± 4.35###
TG (mg/dL)	78.25 ± 3.57	119.80 ± 27.03	79.25 ± 2.46	72.50 ± 5.81	85.75 ± 4.66	98.25 ± 7.09
HDL (mg/dL)	50.88 ± 6.46	65.00 ± 3.24	52.25 ± 2.46	44.75 ± 5.19	56.75 ± 7.87	53.00 ± 1.17
LDL (mg/dL)	38.63 ± 9.22	54.98 ± 8.40	43.75 ± 4.66	31.30 ± 9.20	44.20 ± 3.83	33.00 ± 4.62
T. lipids (mg/dL)	274.1 ± 11.61	385.7 ± 25.07***	285.4 ± 11.58	241.3 ± 3.35	304.3 ± 11.24##	291.8 ± 9.100##

levels. It is noteworthy that MEE had a strong inhibitory effect MDA and GPx in the kidney tissue. Furthermore, high-dose MEE (100 mg/kg) significantly elevated hepatic levels for SOD, GSH, and CAT above control values ($p < 0.05$), suggesting a dose-dependent antioxidant protective effect.

3.11 Tissue accumulation of TiO_2 nanoparticles

Inductively coupled plasma mass spectroscopy (ICP-MS) analysis revealed that rats administered TiO_2NPs at a dose of 300 mg/kg bw/day exhibited a significant increase in Ti accumulation in both hepatic and renal tissues over the 14-day exposure period (Table 9).

ICP-MS was used to assess the levels of TiO_2NPs (µg/g of tissue). Three attempts were made at each measurement. Data are displayed as mean ± SE (n = 5). Significant changes from the control group are indicated by * $p < 0.05$; ** $p < 0.001$; *** $p < 0.0001$, and significant differences from the TiO_2NPs group are indicated by # $p < 0.05$; ## $p < 0.001$; ### $p < 0.0001$.

3.12 Influence of MEE on histopathology in rats treated with TiO_2NPs

Liver slices of control and those treated with MEE50 exhibited normal hepatocytes displaying intact cytoplasm and slightly dilated sinusoids radiating from central vein with (Fig. 7B). In MEE100 treated animals, hepatocytes polyhedral cells appeared with acidophilic, finely vacuolated cytoplasm, central rounded vesicular nuclei with prominent nucleoli, and normal sinusoids between hepatocytes (Fig. 7C). Conversely, liver HE-stained sections from TiO_2NPs-exposed rats displayed significant histological alterations, including complete loss of normal hepatic cord architecture, marked hepatic necrosis, multi-vacuolation, and infiltration of mononuclear cells within dilated hepatic sinusoids (Fig. 7D). Rats co-treated with TiO_2NPs plus MEE50 demonstrated partial hepatic recovery, evidenced by reduced apoptosis and inflammatory infiltration with darkly stained nuclei. Remarkably, the liver of group receiving TiO_2NPs plus MEE100 maintained normal architecture of the hepatic cords and histological appearance, indicating a protective effect of the higher MEE dose.

Kidney HE-stained sections from control animals displayed normal structure of kidneys including, intact glomerulus surrounded by Bowman's capsule and capsular space, a clearly defined vascular pole, and a well-preserved normal proximal and distal convoluted tubules lined with low cuboidal epithelial cells (Fig. 8A). Rats given MEE50 had kidney cortex slices revealed nearly normal renal tissue, with little inflammatory infiltration surrounding the glomeruli (Fig. 8B). Similarly, kidney cortex of mice given MEE100 displayed well-preserved Bowman's capsule, glomeruli, and renal tubules,

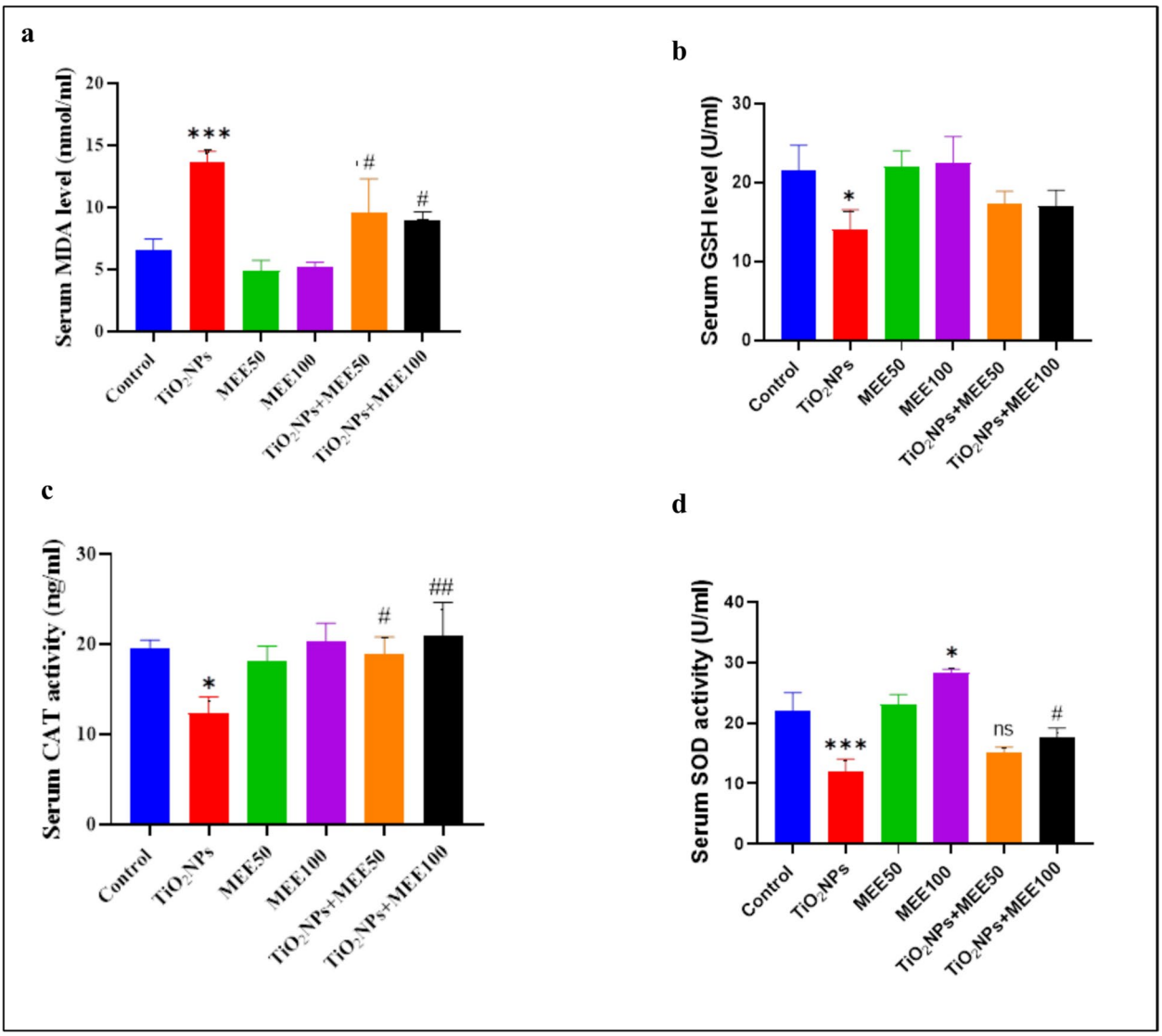


Fig. 4 Effect of MEE on hepatic oxidative stress markers in rats given TiO_2NPs. Parameters assessed include: **a** malondialdehyde (MDA), **b** reduced glutathione (GSH), **c** catalase (CAT), **d** superoxide dismutase (SOD). Data are presented as mean ± SE (n = 5). Statistical analysis was performed using one-way ANOVA followed by Tukey's test. Symbols indicate significant differences: $^{*}P < 0.05$ versus control group; $^{\#}P < 0.05$ versus TiO_2NPs-treated group

indicating minimal histological alterations (Fig. 8C). In contrast, TiO_2NPs-treated rats showed marked renal damage including, glomerular tuft congestion, bleeding, tubular dilation, interstitial edema, and lymphocytic infiltration surrounding both glomeruli and renal tubules (Fig. 8D). Animals treated with TiO_2NPs and MEE at both doses revealed partial restoration of renal architecture, with normal glomerular tufts and only mild cloudy swelling in some tubules. Notably, rats treated with TiO_2NPs and MEE100 indicated substantial improvement in kidney histology (Fig. 8F), suggesting a protective effect of the higher MEE dose.

When the control animals' heart sections were examined, they showed normal nuclei and longitudinal cardiac muscle fibers that were well organized. The heart of rats treated with both doses of MEE displayed a normal appearance, with well-organized longitudinal cardiac muscle fibers and normal nuclei (Fig. 9C and D). The nano-titanium treated group exhibited focal perivascular mild fibrosis infiltrated by a few leukocytes. In addition, there is evidence of hyalinization and vacuolation of cardiac muscle fibers, as well as disorganization of the cardiac muscle fibers and congested cardiac blood vessels. Animals given TiO_2NPs + MEE50 had modest clogged

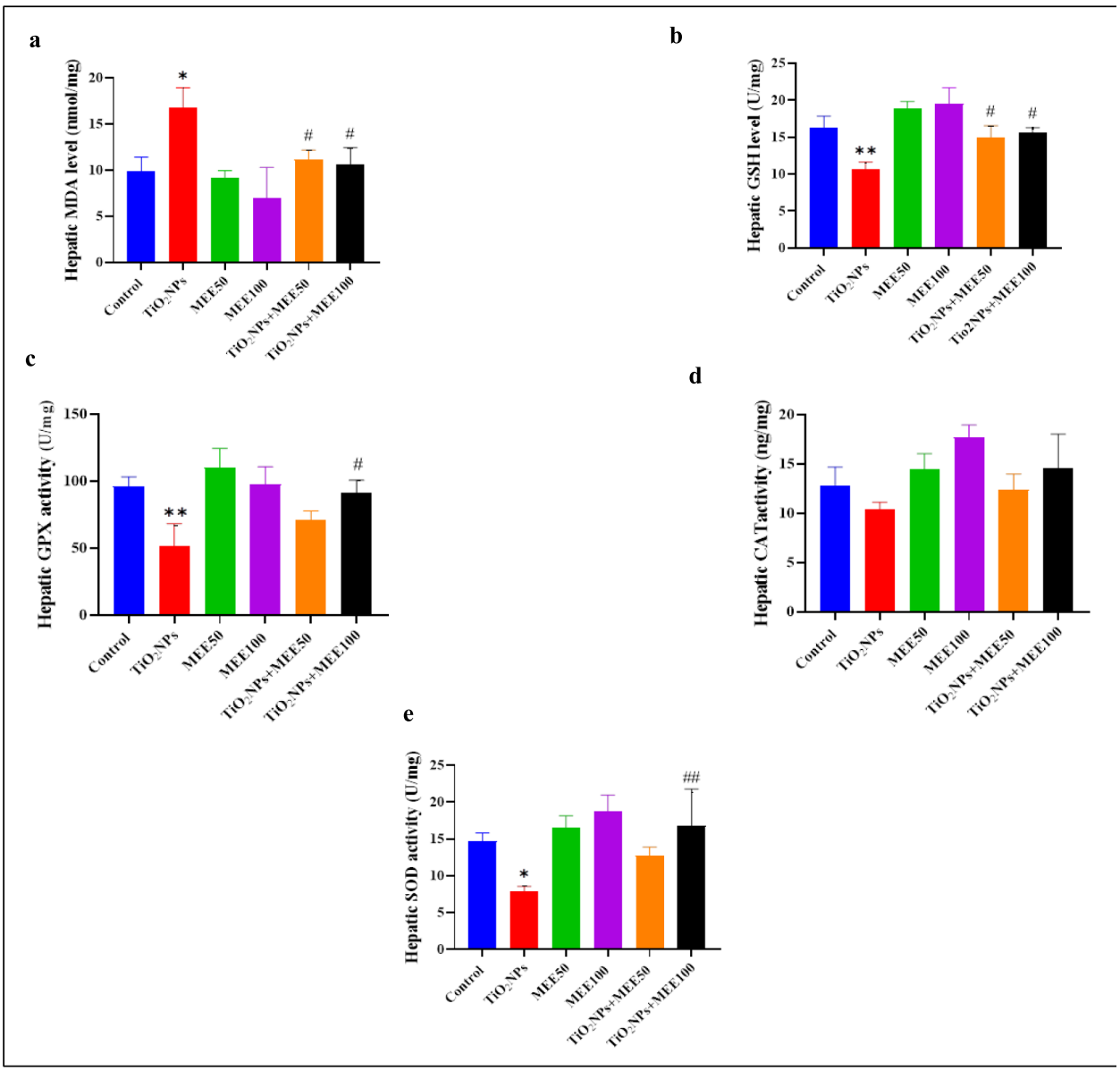


Fig. 5 Effect of MEE on serum oxidative stress markers in rats given TiO_2NPs. Parameters assessed include: **a** malondialdehyde (MDA), **b** reduced glutathione (GSH), **c** catalase (CAT), **d** superoxide dismutase (SOD). Data are presented as mean ± SE (n = 5). Statistical analysis was performed using one-way ANOVA followed by Tukey's test. Symbols indicate significant differences: $^{*}P < 0.05$ versus control group; $^{\#}P < 0.05$ versus TiO_2NPs-treated group

cardiac blood arteries in their hearts, but their cardiac muscle fibers and nuclei remained normal (Fig. 9E). Meanwhile, TiO_2NPs plus MEE 100 showed normal appearance with well-organized longitudinal cardiac muscle fibers (Fig. 9F).

Figure 10A1 & A2 illustrates that the testes of control rats displayed a normal arrangement of somniferous tubules with germ epithelial cells, including numerous spermatogonia featuring normal nuclei with many mature spermatozoa present. Organization of spermatogenic cells in the testes of rats that given both doses of MEE appeared normal, with multiple phases of germ cell maturation and plentiful mature spermatozoa (Fig. 10C1, C2, D1 & D2). Necrosis in several layers of spermatogenic germ cells—predominantly impacting spermatogonia and primary spermatocytes, resulting in testicular architecture in rats treated with TiO_2NPs. Clumps of sloughed germ cells were observed within

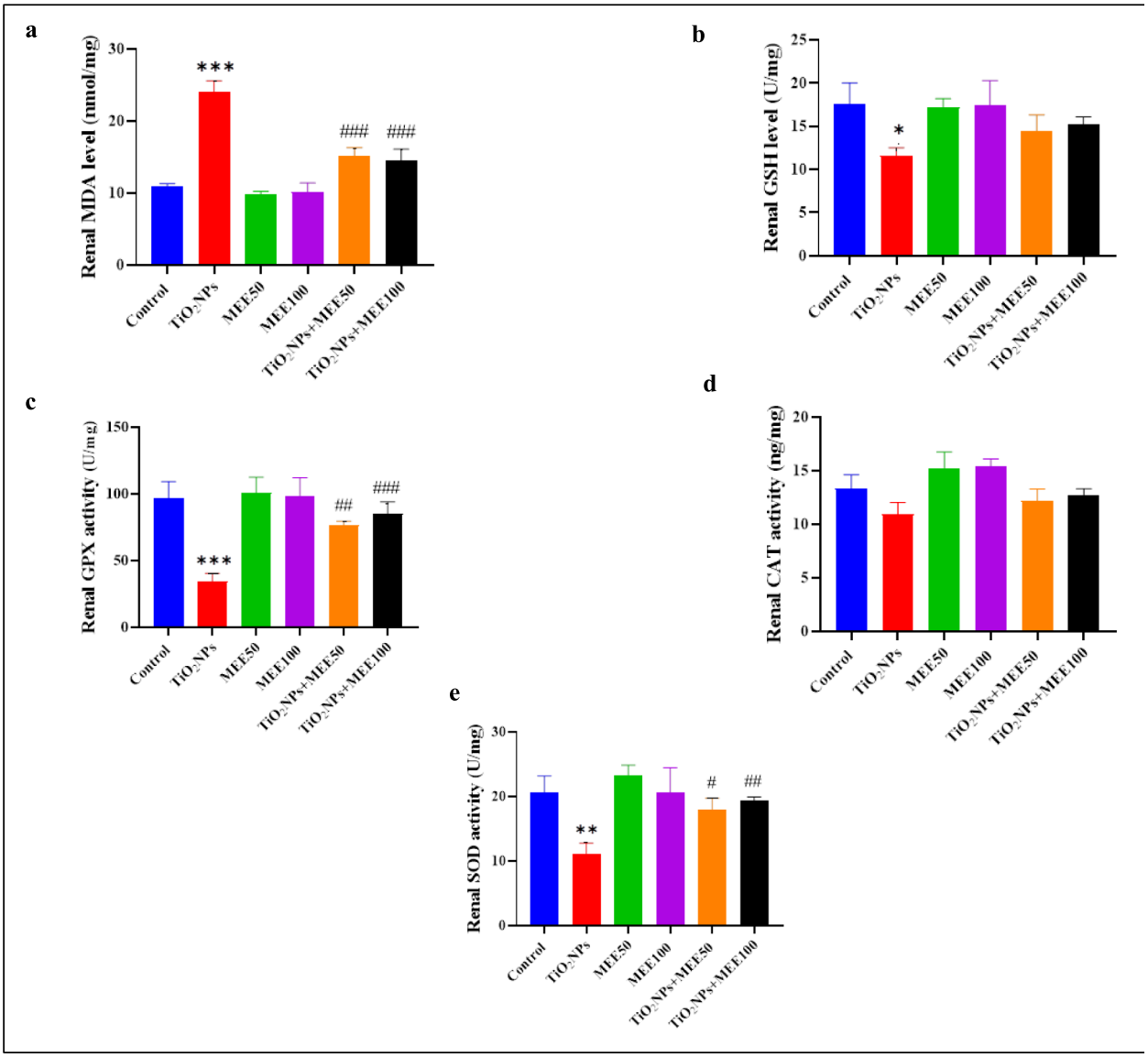


Fig. 6 Effect of MEE on renal oxidative stress markers in rats given TiO_2NPs. Parameters assessed include: **a** malondialdehyde (MDA), **b** reduced glutathione (GSH), **c** catalase (CAT), **d** superoxide dismutase (SOD). Data are presented as mean ± SE (n = 5). Statistical analysis was performed using one-way ANOVA followed by Tukey's test. Symbols indicate significant differences: $^{*}P < 0.05$ versus control group; $^{\#}P < 0.05$ versus TiO_2NPs-treated group

Table 9 Levels of TiO_2NPs (µg/g of tissue) in liver and kidney tissues

Parameters	Titanium (µg/g liver tissue)	Titanium (µg/g in kidney tissue)
Control	0.0 ± 0.00	0.00 ± 0.00
TiO_2NPs	52.40 ± 0.81****	62.00 ± 0.07****
TiO_2NPs + MEE50	23.00 ± 0.71$^{\#\#\#\#}$	19.40 ± 0.51$^{\#\#\#\#}$
TiO_2NPs + MEE100	14.00 ± 0.71$^{\#\#\#\#}$	4.80 ± 0.37$^{\#\#\#\#}$

the tubular lumen, indicative of degenerative changes in the testis; this included severe vacuolation and pyknosis of spermatogonia, and significant eosinophilic necrotic debris occluding the tubular lumen (Fig. 10B1 & B2). The treated animals with TiO_2NPs plus MEE50 exhibited a slightly normal structure of germ epithelial cells, with some spermatocytes showing intracellular vacuolation and a thinning of the spermatogenic epithelium, while those treated with TiO_2NPs plus MEE100 exhibited a regular arrangement of spermatogenic cells within the seminiferous tubules, with clear evidence of multiple

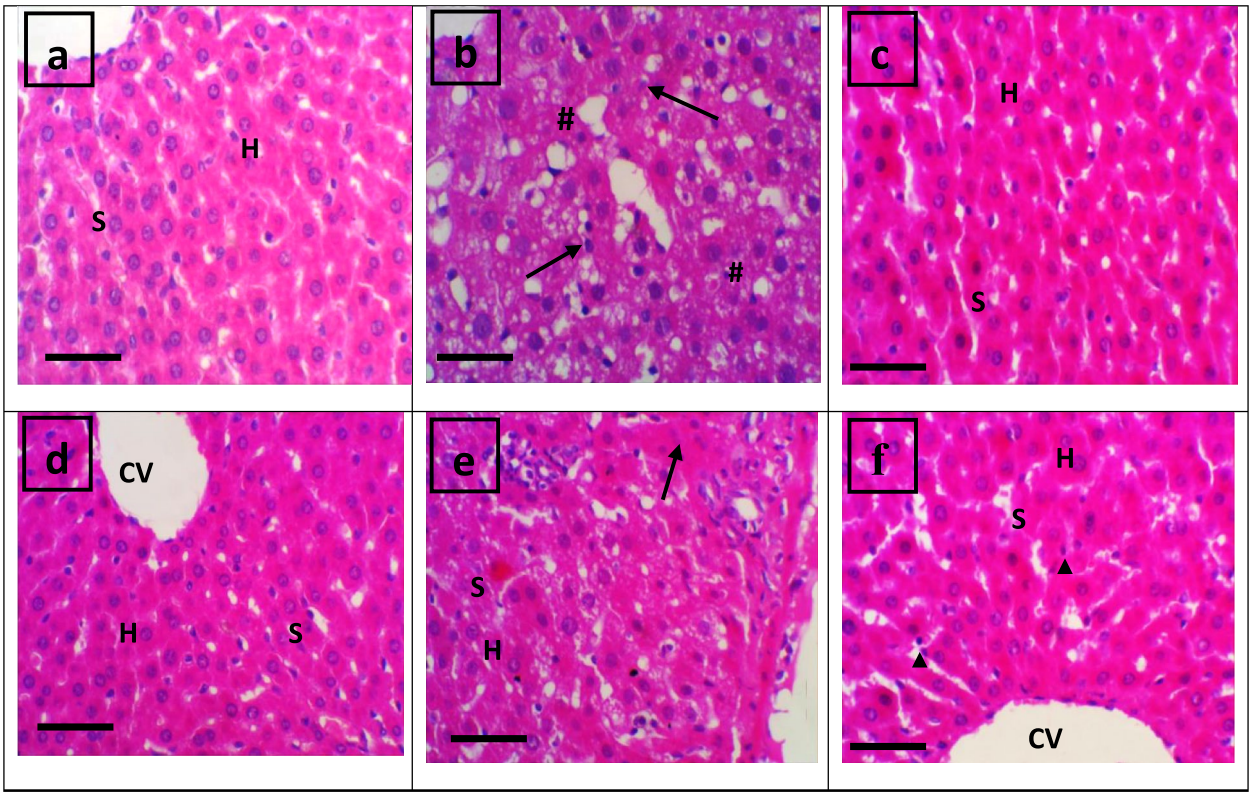


Fig. 7 Photomicrograph of a liver paraffin section from the experimental and control groups: **a** Control group exhibits typical hepatic cell aggregation and normal liver tissue histopathology. Hepatic sinusoids (S) divide the rows of normal hepatocytes (H), which are elevated from the normal central vein (CV). **b** The TiO_2NPs group shows obvious hepatic necrosis (black arrow), multi-vacuolation (#), and hepatic sinusoidal dilatation, along with a total loss of normal hepatic cord architecture. **C** Normal polyhedral hepatocytes (H) in the high-dose group have central rounded vesicular nuclei with prominent nucleoli and acidophilic coarsely vacuolated cytoplasm. Normal sinusoids appear in between hepatocytes (S). **D** Low-dose group normal hepatocyte (H) raised from normal central vein (CV), with slightly dilated sinusoids (S). **e** TiO_2NPs + low dose showing fine and partial improvement of hepatic tissue with still presence of apoptotic hepatocyte (black arrow) and inflammatory infiltration with darkly stained nucleus. **f** TiO_2NPs + high-dose-only hepatic cord preserves its normal architecture and histological appearance. Nearly normal hepatocytes (H) and sinusoids (S) appear more or less normal; The sinusoids are lined with Kupffer cells (arrow head) for regeneration. Magnification X: 400. scale bar 50 µm

maturation stages and overall preservation of testicular architecture.

4 In Silico ADMET profiling of phytoconstituents from *M. crystallinum*

4.1 ADME analysis of tested phytochemicals in Silico

Poor ADMET features can compromise the therapeutic potential of otherwise promising drug candidates. Among the major challenges in drug discovery, particularly during clinical trials, are unfavorable pharmacokinetic properties, which significantly increase the cost of development. To assess the potential of *M. crystallinum* ethanolic crude extract as a viable candidate for drug development, ADMET parameters were estimated using in silico tools (Tables 10 and 11). The majority of the identified phytoconstituents complied with Lipinski's rule of five, and several of them demonstrated a good bioavailability score by passing the Ghose, Veber, and Egan filters. Solubility is another essential factor that affects a compound's distribution and absorption in the body. Notably, most compounds demonstrated higher water solubility, further supporting their potential for oral bioavailability (Fig. 11).

4.1.1 Toxicity profiling of screened phytochemicals using in silico tools

Complementary in silico toxicity assessment introduces an effective approach to reduce reliance on animal testing, as well as the cost and time, supporting ethical research practice. As outlined in Table 11, inhalational and oral toxicity of selected phytochemicals from M. *crystallinum* was predicting using software (ProTox-II). The four compounds exhibited no toxicity under either inhalation or oral route and were classified as class four, indicating low acute toxicity. Linoleic acid was classified as class six in toxicity, reflecting an even lower toxicity

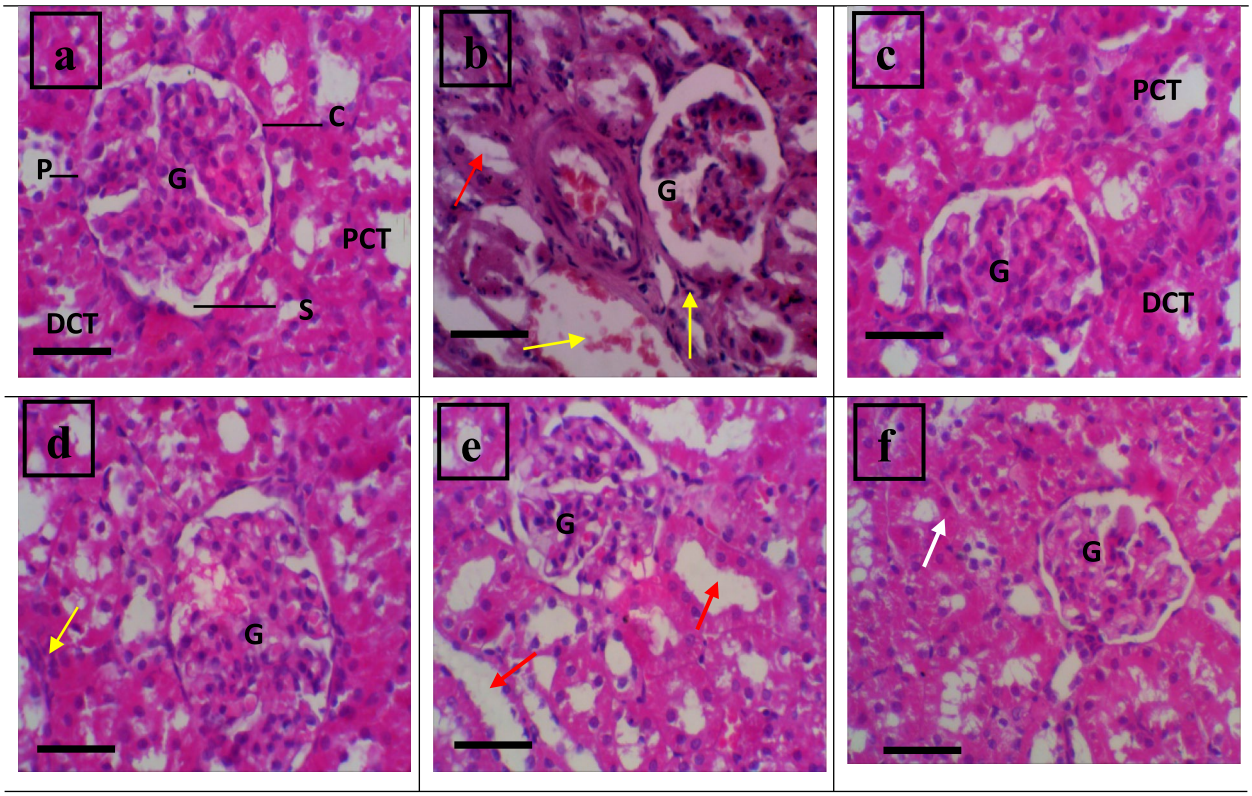


Fig. 8 The control group's paraffin section of the rat kidney, which includes the vascular pole (P), normal proximal convoluted tubule (PCT), normal distal convoluted (DCT), and normal glomerulus (G) surrounded by its glomerular capsule (**c**) and capsular space (S), is shown in the photomicrograph of the kidney. **b** The group of TiO_2NPs exhibiting severe glomerular tuft bleeding and congestion (G), renal tubule enlargement (red arrow), and interstitial tissue edema with lymphocytic cell infiltration surrounding glomeruli and renal tubules (yellow arrows). **c** High-dose group showing normal glomeruli (G) having a well-structured Bowman's capsule as well as distal (PCT) and proximal (DCT) convoluted tubules. **d** The renal tissue of the low-dose group shows tiny infiltration surrounding the glomeruli, appearing almost normal (yellow arrow). **e** TiO_2NPs + low dose with a glomerular tuft that is almost normal (G) and some tubules that have hazy swelling (red arrow). **f** The kidney histological architecture improved with TiO_2NPs + high dose, approximating the control group with little swelling cells (white arrows). 400 times magnification. scale bar 50 µm

potential. The predicted LD50 values further supported these findings: D-Pinitol, pentakis (trimethylsilyl) ether was 1500 mg/kg, palmitic acid, TMS derivative and stearic acid, TMS derivative was 2280 mg/kg, and linoleic acid, TMS derivative was 20,000 mg/kg. Taken together, these results suggest that the evaluated compounds possess favorable safety margins, supporting their candidacy for further pharmacological investigation and potential therapeutic application.

5 Discussion

The current study provides a comprehensive into the phytochemical profile and biological properties of *M. crystallinum* cultivated in North Sinai, Egypt, and explores its potential to mitigate the toxicity of TiO_2NPs. The findings confirm that *M. crystallinum* is a rich source of bioactive compounds and possesses strong antioxidants, non-cytotoxic, and organo-protective properties, making it a valuable candidate for use in food and pharmaceutical applications.

Numerous studies have confirmed that *M. crystallinum* has a variety of bioactive chemicals influenced by the weather, climate, soil, and care circumstances [47]. Our results, consistent with previous research, revealed that the ethanolic extract of *M. crystallinum* is abundant with flavonoids, phenolics, saponins, and tannins as well as alkaloids, chlorophylls, and carotenoids [23, 24, 47]. Previous report have identified 23 polyphenolic components, with catechin (41.15%), pyrogallol (7.30%), and catechol (6.59%) as most abundant [47] aligns with studies linking these compounds to numerous health benefits such as free radicals scavenging, carcinogenesis prevention, and immune system enhancement [48].

The antioxidant power was assessed by IC50. The *M. crystallinum* extract recorded 23.79 ± 1.03 compared to ascorbic acid 76.12 ± 3.24. Lower IC50 values indicate higher activity; hence, the extract demonstrated potent

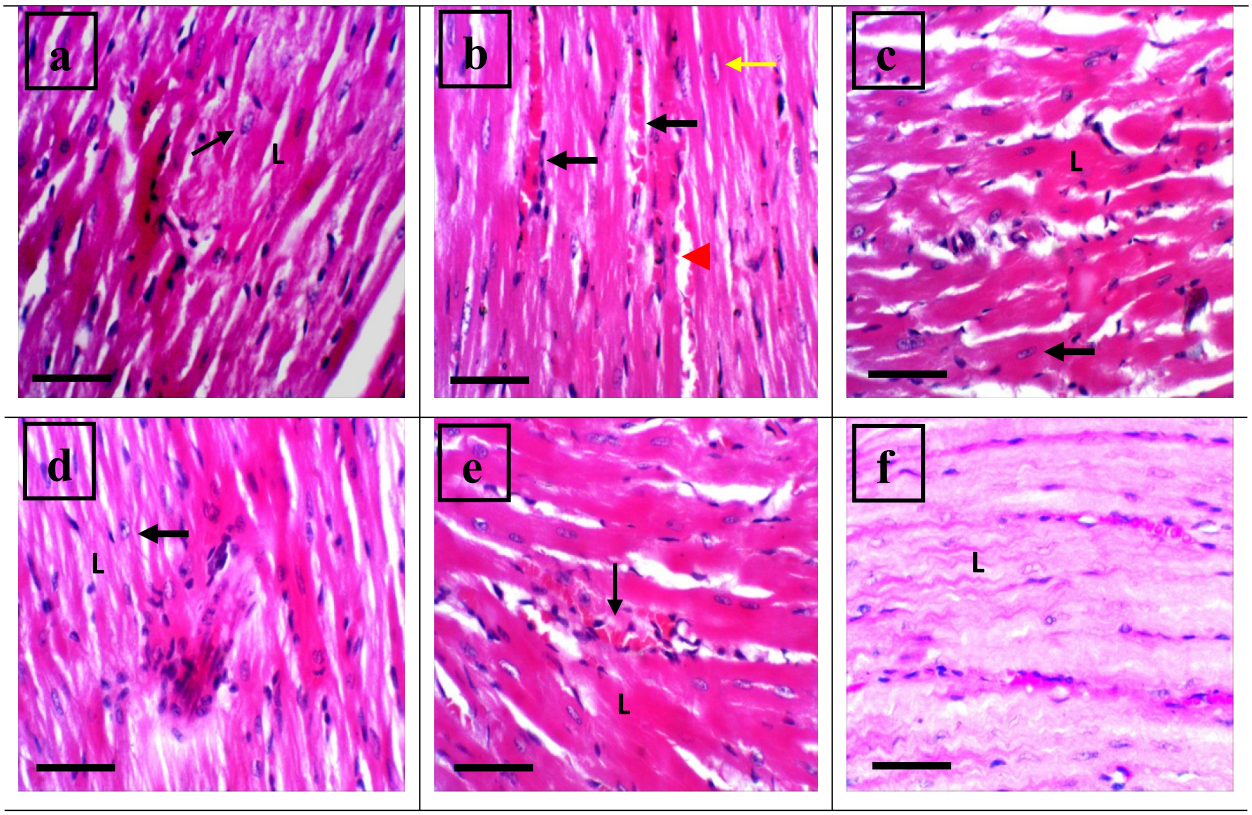


Fig. 9 A photomicrograph a paraffin section of treatments and control groups hearts. **a** Demonstrates that the control group longitudinally (L) cardiac muscle fibers are well organized and have a normal nucleus (black arrow). **b** Nano-titanium group shows focal perivascular mild fibrosis infiltrated with few leukocytes (black arrow), demonstrating hyalinization and vacuolation (yellow arrows) of cardiac muscle fibers, disorganization of cardiac muscle fibers (arrow head) and congested cardiac blood vessels (black arrows). **c** High-dose group and **d** low-dose group normal showing normal appearance and well organization of longitudinally (L) cardiac muscle fibers with normal nucleus (black arrow) in both groups. **e** Nano-Ti + low dose shows mildly congested cardiac blood vessels (black arrow) and normal cardiac muscle fibers with normal nucleus. **f** Nano-Ti + high dose only showing nearly normal appearance and well organization of longitudinally (L) cardiac muscle fibers. Magnification X: 400. scale bar 50 µm

antioxidant capacity attributed to its flavonoids and polyphenols [48]. This highlights its potential use in food and pharmaceutical industries.

The BHK-21 cell line derived from Syrian hamster's kidney cells was used to assess *M. crystallinum's* cytotoxicity. The result showed that *M. crystallinum* exhibited a CC50 value of 281.32 ± 8.94 µg/mL. This value is critical as it represents the concentration at which half of the cell population is inhibited or killed. According to the criteria set by The American National Cancer Institute (NCI), a botanical extracts are cytotoxic if IC50 is less than 20 µg/mL [49]. Based on this criterion, *M. crystallinum* can be considered a non-cytotoxic plant.

The GC analysis further enriched our understanding of the plant's active constituents. The high abundance of ester (> 50) and ether compounds (32.6%) particularly, linoleic acid (LA) and D-Pinitol, reveals the mechanistic basis for the observed biological effects. LA represents 33% of the *M. crystallinum* components that enhance CD8 + T cell metabolic fitness and antitumor immunity but may promote inflammation and metabolic diseases when consumed in excess [50]. Ether compounds showed bactericidal, fungicidal, antidepressant, anticancer, and herbicidal properties. Similarly, D-Pinitol (20.5%) is a well-documented compound with potent antidiabetic, anti-inflammatory, antioxidant, anticancer, hepatoprotective, cardioprotective, and neuroprotective benefits [25, 51]. The synergistic action of these compounds likely contributes to the plant's overall therapeutic efficacy.

Our investigation into the toxicity of TiO_2NPs supports established literature reporting their adverse effects on multiple organs and metabolic processes [55, 56]. The gastrointestinal tract is recognized as the primary route of absorption, and particle size strongly affects pharmacokinetics, tissue distribution, and clearance. Nanoparticles within 50–300 nm range are considered optimal for absorption [52]. In this study, TiO_2NP were spherical and

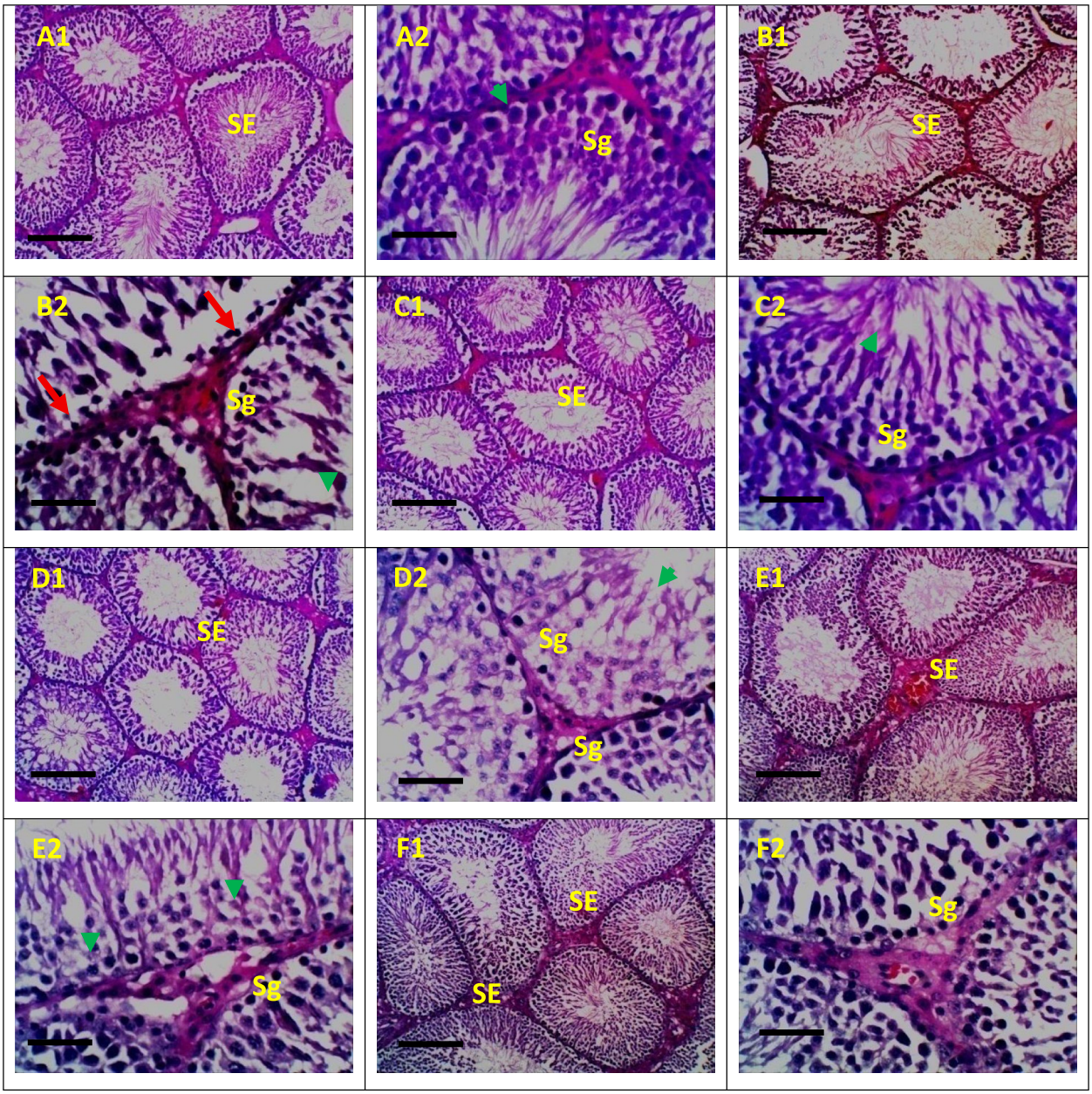


Fig. 10 A paraffin segment of the testis from the experimental and control groups is photomicrographed: (**A**1, **A**2) The control group exhibits a typical seminiferous tube (SE) arrangement of germ epithelial cells, with mature spermatozoa and a large number of spermatogonia (Sg) with normal nuclei (arrowhead). (**B**1, **B**2) Nano-titanium group observed. Several spermatogenic germ cell layer necrosis (mostly in spermatogonia and primary spermatocytes) and altered testicular architecture testicular degenerative abnormalities, such as severe spermatogonia vacuolation with spermatogonial pyknosis (green arrows), and noticeable eosinophilic necrotic debris obstructing the tubular lumen (arrowhead), are evident in the admixed intraluminal clumped sloughed germ cells. The spermatogenic cells in the (**C**1, **C**2) high-dose group are arranged normally, and there are numerous mature spermatozoa (arrowhead) at different stages of maturation. (**D**1, **D**2) Low-dose group showing a typical spermatogenic cell arrangement with several mature spermatozoa (arrowhead) and different phases of maturation. (**E**1, **E**2) Nano-Ti + low dose exhibiting intracellular vacuolation, spermatocytes, germ epithelial cells, and spermatogenic epithelium thinning with a slight normal structure (arrowhead). (F1, F2) Nano-Ti + high dose showing diverse levels of germ cell maturation throughout the germ cell layer in the testicular architecture, together with a regular arrangement of spermatogenic cells (Sg) in the seminiferous tubules. (Image magnification X: 200 for A1, B1, C1, D1, E1, and F1. X: 400 for A2, B2, C2, D2, E2, and F2). scale bar 50 µm

Table 10 Predictive ADME analysis of bioactive phytochemicals via in silico tools

Descriptors	D-Pinitol, pentakis(trimethylsilyl) ether	Palmitic Acid, TMS derivative	Linoleic acid, TMS	Stearic acid, TMS derivative
SMILE	COC1C(C(C(C(C1O[Si](C)(C)C)O[Si](C)(C)C)O[Si](C)(C)C)O[Si](C)(C)C)O[Si](C)(C)C	CCCCCCCCCCCCCCCC(=O)O[Si](C)(C)C	CCCCC/C=C\C/C=C\CCCCCCCC(=O)O[Si](C)(C)C	CCCCCCCCCCCCCCCCCC(=O)O[Si](C)(C)C
Physicochemical properties				
Number of heavy atoms	33	22	24	24
Number of aromatics heavy atoms	0	0	0	0
Fraction Csp3	1	0.95	0.76	0.95
Number of rotatable Bonds	11	16	16	18
Number of H-bond acceptors	6	2	2	2
Number of H-bond donors	0	0	0	0
Molar refractivity	151.60	102.60	111.27	112.21
Topological polar surface area (Å2)	55.38	26.30	26.30	26.30
Lipophilicity				
Log Po/w (iLOGP)	5.50	5.33	0	6.01
Log Po/w (XLOGP3)	6.63	8.87	0	9.95
Log Po/w (WLOGP)	6.12	6.85	7.18	7.63
Log Po/w (MLOGP)	1.14	4.91	0	5.36
Log Po/w (SILICOS-IT)	-3.03	5.30	0	6.17
Consensus log Po/w	3.27	6.25	0	7.02
Water solubility				
Log S (ESOL)	− 6.73	6.41	0	− 7.13
Solubility (mg/ml)	1.03e−04	1.28e−04	–	2.63e-05
Class	Poorly soluble	Poorly soluble	–	Poorly soluble
Log S (Ali)	− 7.59	− 9.31	–	− 10.43
Ali Solubility (mg/m	1.41e-05	1.62e−07	–	1.33e−08
Class	Poorly soluble	Poorly soluble	–	Insoluble
Log S (SILICOS-IT)	− 5.08	− 6.86	–	−7.65
Solubility	4.63e−03	4.50e-05	–	7.91e-06
Class	Moderately soluble	Poorly soluble	–	Poorly soluble
Pharmacokinetics				
GI absorption	High	Low	-	Low
BBB permeant	No	No	–	No
P-gp substrate	No	No	–	No
CYP1A2 inhibitor	No	Yes	–	Yes
CYP2C19 inhibitor	No	No	–	No
CYP2C9 inhibitor	No	No	–	No
CYP2D6 inhibitor	No	No	–	No
CYP3A4 inhibitor	No	No	–	No
Log Kp (skin permeation) (cm/s)	− 4.98	− 2.01	–	-1.41
Drug-likeness				
Lipinski	1	1	0	1
Ghose	4	1	–	1
Veber	1	1	–	1
Egan	1	1	–	1

Table 10 (continued)

Descriptors	D-Pinitol, pentakis(trimethylsilyl) ether	Palmitic Acid, TMS derivative	Linoleic acid, TMS	Stearic acid, TMS derivative
Muegge	1	2	–	2
Bioavailability score	0.55	0.55	–	0.55
Medicinal chemistry				
PAINS	0	0	0	0
Brenk	1	1	0	1
Lead likeness	3	2	–	3
Synthetic accessibility	7.34	4.53	–	4.77

Table 11 Analysis of phytochemicals that resemble 50% of the MEE in terms of in silico toxicity

No	Phytochemicals	Oral toxicity of phytochemicals (ProTox-II)		Acute inhalation toxicity	Acute oral toxicity
		Predicted LD50 (mg/kg)	Predicted toxicity class		
1	D-Pinitol, pentakis (trimethylsilyl) ether	1500	4	Non-toxic (59.0%)	Non-toxic (81.0%)
2	Palmitic Acid, TMS derivative	2280	4	Non-toxic (71.0%)	Non-toxic (92.0%)
3	Linoleic acid, TMS	20,000	6	Non-toxic (75.0%)	Non-toxic (93.0%)
4	Stearic acid, TMS derivative	2280	4	Non-toxic (71.0%)	Non-toxic (92.0%)

measured between 10 and 50 nm, which is smaller than the ideal size for efficient mucosal uptake.

For in vivo investigation, TiO_2NPs with a crystallite size of < 50 nm were administered orally for 14 days at dose of 300 mg/kg bw/day. According to EFSA (2021), repeated oral administration of TiO_2NPs has been linked to adverse health outcomes in animal models. Similar to studies reports body weight reduction in Wistar albino rats, male SD, and CD-1 mice [55], our finding revealed reduced body weight gain in treated rats compared to control. Evidence suggests that nanoparticles ingestion disturbs digestion and food absorption, resulting in a shortage of vital macronutrients and micronutrients that ultimately alter body weight [56]. In mice, given varied doses of TiO_2NPs have also been linked to loss of appetite, further contributing to body weight reduction [16]. Moreover, histological analysis demonstrated a decrease in intestinal villi number, thereby reducing absorptive surface area, impairing nutrients uptake, and further contributing to malnutrition induced body weight loss [17].

The results indicated that TiO_2NPs administration led to abnormal hematological and physiological changes in male rats. Although no discernible variations were detected in the absolute numbers of leukocyte subtypes or total leukocyte counts, the minor alterations were observed in leukocyte fraction during the 14-day exposure considered of limited toxicological importance [57]. In contrast, marked abnormalities were evident in biochemical parameters. These included significant decrease in total protein, albumin, HDL, and antioxidant enzyme activity, alongside pronounced increase in liver, kidney, and cardiac function indices, oxidative marker MDA, cholesterol, TG, and LDL levels. Collectively, these findings clearly showed that TiO_2NPs exposure disrupts hepato-renal function, leading to detrimental alterations in blood biochemical markers. Prior studies support these outcomes, reporting that rats exposed to TiO_2NPs had significantly higher blood urea, creatinine, ALT, AST, T. bilirubin, and uric acid levels compared to the control group. Such elevations are indicative of renal impairment, likely resulting from reduced glomerular filtration rate. Since the liver and kidneys are primary targets of xenobiotics metabolism and detoxification, they appear to be particularly susceptible to nanoparticle toxicity. Sub-acute injection TiO_2NPs has further been associated with dyslipidemia, renal dysfunction, hyperglycemia, and increased liver enzyme activity. In a similar vein, acute exposure studies revealed oxidative damage and adverse alterations in serum, hepatic, and renal biomarkers in adult male rats following 14 consecutive days of TiO_2NPs administration [58, 59]. Moreover, disruption of lipid homeostasis was evident, as TiO_2NPs administration significantly elevated TG, cholesterol, and LDL levels while reducing HDL. This imbalance indicates that the nanoparticles interfere with the lipoprotein metabolism and lipid

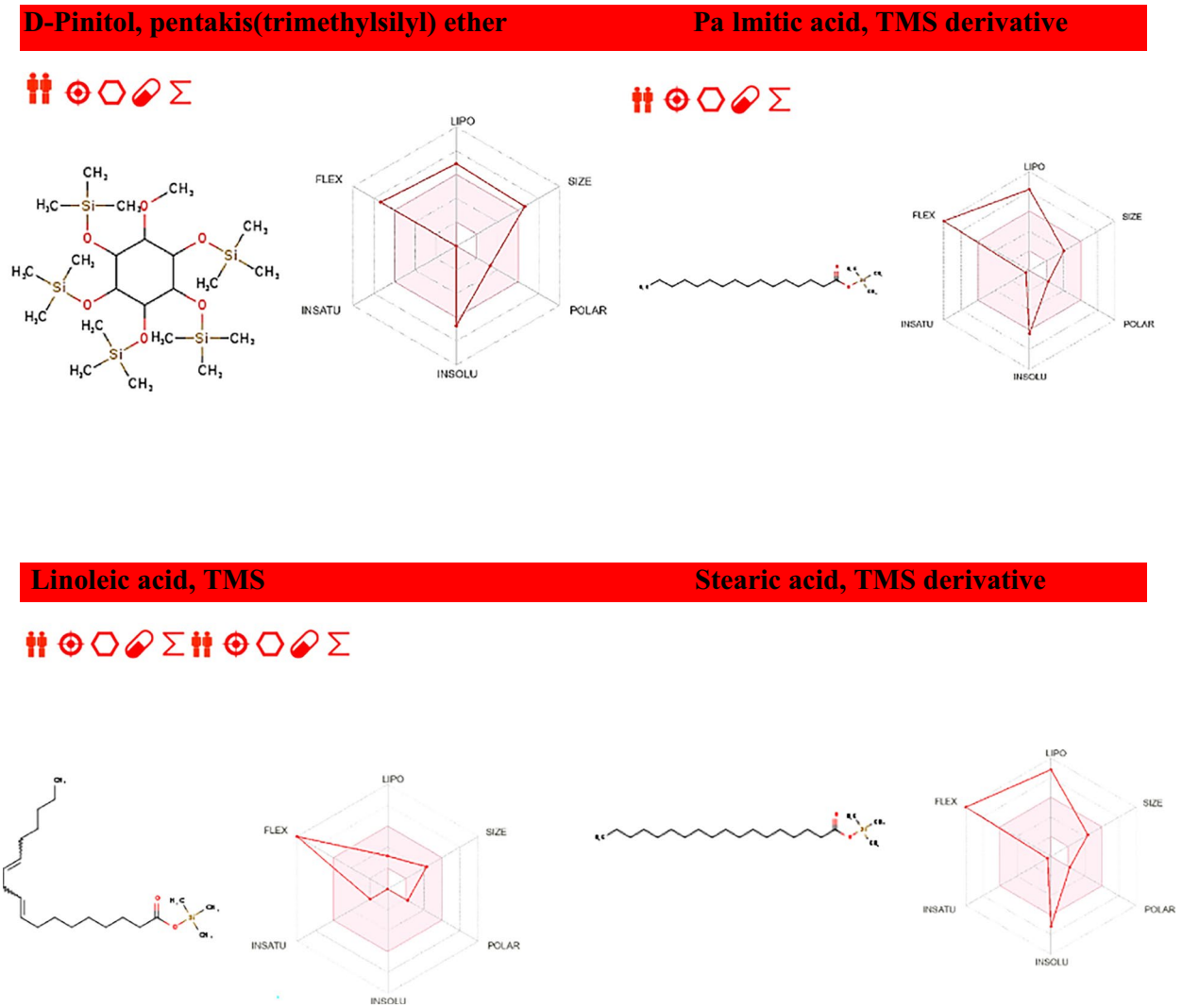


Fig. 11 D-pinitol, stearic acid, palmitic acid, pentakis (trimethylsilyl) ether, linoleic acid, TMS, and TMS derivative bioavailability radars

transport [17]. Furthermore, cardiovascular disorders and other metabolic syndromes are linked to elevated TG and cholesterol levels and given the established role of LDL in promoting arteriosclerosis, TiO_2NPs may also represent a potential risk factor for cardiovascular diseases. Supporting this, similar outcomes have been observed in rats exposed to TiO_2NPs [49].

The present study reinforces the well-established role of oxidative stress as a central mechanism underlying the toxicity of TiO_2NPs. Numerus studies have demonstrated that TiO_2NPs are potent inducers of reactive oxygen species (ROS), which initiate a cascade of cellular damage [60].

Among these ROS, hydroxyl radicals (•OH) are particularly potent and are considered the primary agents responsible for oxidative damage caused by TiO_2NPs [61].

One of the earliest manifestations of ROS-induced damage is lipid peroxidation (LP), which alters the structural integrity of cell membranes and disrupts essential cellular functions. Rajapakse et al. [62] demonstrated that oral exposure to TiO_2NPs due to the production of •OH, which starts oxidative stress and causes lipid abnormalities, accumulation of malondialdehyde (MDA), and a marked reduction in the hepatic antioxidant capacity. In particular, glutathione (GSH), a key intracellular antioxidant, was significantly depleted indicating compromised redox regulation in the liver.

Further evidence of systemic oxidative stress is reflected in decreased levels of antioxidants in serum, liver, and kidney tissues, accompanied by elevated MDA level. These biochemical alterations suggest oxidative damage and impaired redox balance across multiple organs; DNA damage as indicated by increased levels of

8-hydroxy-2'-deoxyguanosine (8-OHdG) in the liver and kidney tissues further supports the role of ROS in genotoxicity [63].

Elevated in MDA and lowering antioxidant enzymes in tissues may also promote cell apoptosis. Shi et al. [64] highlighted the critical role of nuclear factor erythroid 2-related factor 2 (Nrf_2) in cellular defense against oxidative stress. Their finding revealed that Nrf_2 deficiency worsens DNA damage and raises the risk of cancer. Moreover, the reduction in SOD activity impairs the detoxification of superoxide radicals which in turn disrupts CAT activity. This enzymatic disruption leads to the buildup of hydrogen peroxide (H_2O_2), a toxic byproduct of normal metabolic processes. Under physiological conditions, CAT converts H_2O_2 into water and oxygen, thereby preventing oxidative injury. However, diminished CAT activity following TiO_2NPs exposure allows H_2O_2 to accumulate, intensifying oxidative stress in liver and kidney tissues [65]. Once enter the body, NPs are transported via the bloodstream and can accumulate in various organs, affecting vital systems such as the lungs, liver, kidneys, and reproductive organs [66]. Orally administered TiO_2NPs can be absorbed through the gastrointestinal tract and transported through lymphatic pathways [67]. Biodistribution studies confirm predominant accumulation in the liver, followed by the kidneys, with slow clearance and long term retention [68, 69].

Histopathological examination reveals inflammatory infiltration, hepatocellular necrosis, and structural disarray in liver tissues [70, 71], while Kupffer cells show heightened sensitivity to oxidative stress [72]. Renal damage includes the accumulation of protein materials in distal tubules and medullary regions [73], and a cardiac tissues display fibrosis and vascular congestion [55]. Testicular degeneration, necrosis of spermatogenic germ cell layers, and vacuolation, further supports multi-organ injury linked to oxidative stress [74]. These findings underscore the potential threat of TiO_2NPs, especially when used as food additives.

Various medicinal plants are utilized to mitigate the toxicity of TiO_2NPs. For instance, ginger (*Zingiber officinale*) contains gingerol and shogaol, both of which have antioxidant properties [53]. Turmeric (*Curcuma longa*) protects cells against inflammation induced by TiO_2NPs. Additionally, allicin and allyl sulfide, which are found in garlic (*Allium sativum*), provide chelating and antioxidant qualities. *Astragalus membranous* and Indica provide polysaccharides and flavonoids with immunomodulatory properties [20, 54]. Hence, *M. crystallinum* in was evaluated for protective effects against TiO_2NPs toxicity.

Despite limited research on *M. crystallinum* in Egypt, emerging evidence highlights its promising role in mitigating oxidative damage, particularly that induced by TiO_2NPs.

Recognized as both a functional food and a medicinal herb, *M. crystallinum* is rich in bioactive compounds, including flavonoids, polyphenols, catechin, catechol, neo-hesperidin, rutin, and hyperoside, and ferulic acid—all known for their potent antioxidant properties [31].

These compounds are essential for scavenging ROS, thereby reducing oxidative stress and protecting cellular integrity. In addition to polyphenolic chemicals, *M. crystallinum* also contains significant antioxidant enzymes. Through their ability to scavenge ROS, these enzymes aid in shielding cells from oxidative damage [75]. D-pinitol, a substance that exhibits a variety biological actions, including anti-inflammatory, anticancer, antidiabetic, and antioxidant benefits, is abundant in *M. crystallinum* [28].

These properties make *M. crystallinum* an excellent candidate for therapeutic applications, especially in conditions associated with inflammation and oxidative stress.

Beyond its antioxidant potential, *M. crystallinum* demonstrates efficacy in metabolic regulation. It has shown significant benefits in managing diabetes and hypertension, and obesity. Studies report that *M. crystallinum* administration in rats led to reduced body attributed to its bioactive lipids, particularly linoleic acid TMS and 2-mono-isobutyrin 2TMS derivative, a glyceride which plays a crucial role in improving lipid metabolism. The presence of myo-inositol further supports its role in preventing fatty liver disease [76].

When co-administered with TiO_2NPs, *M. crystallinum* improved liver, kidney, and heart functions. GC analysis identified hepatoprotective compounds such as palmitic acid and linoleic acid, which reduce oxidative stress and support liver health. D-Pinitol also contributes to lowering liver enzymes and enhancing liver function [33]. Additionally, *M. crystallinum* includes 17-octadecynoic acid, which has anti-inflammatory properties and can help maintain renal function, while 2-oxovaleric acid and 12-benzisothiazole exhibit antioxidant qualities in renal tissues [77].

Cardiac protection is facilitated by 2-mono-isobutyrin 2TMS derivative, which supports energy metabolism and reduces CK activity. Additionally, the (2-butoxyethoxy) acetic acid TMS derivative may help preserve integrity of heart muscle and regulate CK level under stress [78].

M. crystallinum also significantly reduces serum cholesterol level when administered with TiO_2NPs, as supported by statistical evidence [79]. Linoleic acid TMS and linolenic acid trimethylsilyl ester contribute to improved lipid profiles by reducing LDL and triglycerides levels while increasing HDL. Although the specific effects of 2-mono-isobutyrin 2TMS derivative on lipid

parameters are less documented, its role in lipid metabolism is noteworthy. The plant's dietary fiber further enhances cardiovascular health by reducing fat absorption, trapping toxin, and promoting healthy gut microbiome [31].

Oxidative stress is a major contributor to chronic, neurodegenerative, and inflammatory diseases [80]. *M. crystallinum* combats this through its rich phenolic chemicals including flavonoids and tannins, which neutralize ROS and prevent damage to proteins, lipids, and DNA. These antioxidant and anti-inflammatory properties are particularly beneficial for liver health, supporting detoxification and maintaining hepatic function [33].

The synergistic effects fiber, bioactive compounds, and antioxidant enzymes in *M. crystallinum* offer comprehensive cellular protection. Its dual role as both food and medicinal herb positions it as a promising natural remedy against environmental toxins like TiO_2NPs. Carotenoids like beta-carotene and lutein reduce oxidative stress in kidney cells, stabilizing enzyme levels and enhancing kidney health [31]. Triterpenoids and saponins further support kidney function by mitigating inflammation and oxidative stress [81].

Histopathological findings confirm the protective efficacy of *M. crystallinum* ethanolic extract (MEE) when co-administered with TiO_2NPs. Biochemical data revealed that MEE effectively ameliorated the oxidative/antioxidant balance disrupted by TiO_2NPs exposure. These results underscore *M. crystallinum* capacity to reduce tissue and cellular damage. The hepatoprotective effects of *M. crystallinum* are largely attributed to its polyphenols and carotenoids, which neutralize ROS and prevent hepatocyte damage.

These compounds also regulate lipid metabolism by modulating genes involved in lipid synthesis, transport, and breakdown. Such regulation helps counteract TiO_2NPs-induced metabolic disruptions and support liver homeostasis. Polyphenols have demonstrated potential in managing liver diseases through their antioxidant and anti-inflammatory actions. Therefore, both polyphenols and carotenoids are important in maintaining liver function [82], while also offering kidney and heart protection [83].

Antioxidants play a critical role in chelating heavy metals and nanomaterials. Administration of *M. crystallinum* at both tested doses significantly reduced TiO_2NPs deposits in the liver and kidney tissues, highlighting its detoxifying potential [84]. The human antioxidant defense system benefits greatly from exogenous non-enzymatic antioxidants, which include vitamins A, C, and E, β-carotene, minerals, and plant polyphenols—which help mitigate oxidative stress, a key contributor to tissue and cellular damage in various disorders [84].

L-arginine (Arg), a semi-essential amino acid found in *M. crystallinum*, plays a vital role in nitric oxide production, vasodilation, immune response, and nitrogen elimination via urea cycle. Arg supplementation has shown to protect against oxidative stress induced by gold nanoparticles, improving oxidative parameters and cellular integrity [87].

Plant extracts such as grape seed extract proanthocyanidins, cinnamon bark extract, and pomegranate peel have demonstrated hepatoprotective properties against nanoparticles toxicity, including TiO_2NPs and silver nanoparticles [89].

Similarly, *M. crystallinum* methanolic extract contain 23 phenolic compounds, including catechin, pyrogallol, catechol, and ellagic acid, with catechin being the most abundant [90]. Ellagic acid has shown nephroprotective effects in rats intoxicated with iron oxide nanoparticles. Flavonoids, like rutin and neo-hesperidin in *M. crystallinum*, contribute to its antioxidative properties. Rutin, for example, reduces oxidative stress in testicular tissue of rats intoxicated with TiO_2NPs. Furthermore, *M. crystallinum* has shown antioxidative activity through the presence of bioactive ingredients [23, 24, 31]. These bioactive compounds collectively support *M. crystallinum*'s protective role against nanoparticles-induced oxidative damage [91].

6 Conclusion

The present study identified 32 distinct compounds in *M. crystallinum* gathered from North Sinai, with ester (55.99%) and ether (32.68%) being the most abundant, followed by glycoside (6.5819%), silane, heterocyclic compound, and epoxide. In vitro analysis using BHK-21 cells demonstrated that MEE extract possesses antioxidant potential comparable to ascorbic acid and exhibits no-cytotoxic plant, supporting its safety profile. In vivo study revealed that the exposure to TiO_2NPs led to significant physiological and biochemical disturbance, including weight loss, impaired liver, heart, and kidney function, altered lipid profiles, and elevated MDA in blood and tissues. Histological examination confirmed damage in hepatic, renal, cardiac, and testicular tissues, along with reduced GSH and antioxidant enzymes levels. However, co-administration of MEE with TiO_2NPs at both tested doses significantly improved antioxidant status and mitigated TiO_2NPs-induced toxicity. The protective effects are attributed to plant's rich composition of bioactive compounds, including 13-octadecenoic acid (E)- TMS derivative, 17-octadecynoic acid TMS derivative, α-D-galactopyranoside methyl 23-bis-O-(trimethylsilyl)-cyclic phenylboronate, and D-Pinitol pentakis (trimethylsilyl) ether. These findings suggest that *M. crystallinum* holds strong potential as a natural therapeutic agent against

oxidative stress and nanoparticles-induced toxicity. Its application in food or medicinal formulation could offer a valuable strategy for preventing oxidative damage and supporting organ health.

6.1 Future work

Although research on *M. crystallinum* in Egypt is still limited, its strong potential in protecting against oxidative damage caused by TiO_2NPs makes it a valuable subject for further investigation. Future studies should explore the effects of MEE using varied doses such as 25, 125, and 200 mg/kg b.w, and over different durations (one or two months). This will help determine the most effective dose and treatment period for improving the functions of the kidneys, liver, heart, and testicular functions affected by TiO_2NPs-induced toxicity. Expanding research in this direction could support the development of *M. crystallinum* as a natural therapeutic agent.

7 Competing interests

The authors declare no competing interests.

Abbreviations

MC	Mesembryanthemum crystallinum
MEE	Mesembryanthemum ethanolic extract
TiO_2NPs	Titanium dioxide Nanoparticles
TEM	Transmission electron microscopy
TAC	Total antioxidant capacity

Supplementary Information

The online version contains supplementary material available at https://doi.org/10.1186/s43088-025-00693-z.

Additional file1 (DOCX 105 KB)

Additional file2 (DOCX 28 KB)

Additional file3 (DOCX 778 KB)

Author contribution

I.A did experimental analyses and prepared figures and tables. H.E and H.M supervised the study. All authors wrote the main manuscript text and reviewed the manuscript.

Funding

This research did not receive any specific grant from funding agencies in the public, commercial, or not-for-profit sectors.

Data availability

The data produced in this research are available by the corresponding authors on reasonable requests.

Declarations

Consent for publication

Not applicable.

Human ethics and consent to participate

Not applicable.

Informed consent

Not applicable.

Working with animals

All animal experiments were approved by the Institutional Animal Ethics Committee, in compliance with national guidelines, under approval number # ARU/SF.12#

Author details

[1]Botany and Microbiology Department, Faculty of Science, Damietta University, New Damietta, Egypt. [2]National Biotechnology Network of Expertise (NBNE), Academy of Scientific Research and Technology (ASRT), Cairo, Egypt. [3]Zoology Dept., Faculty of Science, Arish University, Al-Arish, North Sinai, Egypt.

Received: 3 June 2025 Accepted: 22 September 2025
Published online: 23 October 2025

References

1. Brindhav AM, Sharma S, Azizi S, Rana VS (2025) Unveiling the cutting-edge applications of nanotechnology in the food industry-from lab to table-a comprehensive review. J Agric Food Res 20:101831
2. Khan, W.S., Asmatulu, E., Asmatulu, R., 2025. Nanotechnology emerging trends, markets and concerns, in: Nanotechnology Safety. Elsevier, pp. 1–21.
3. Musee, N., Sikhwivhilu, L., Gulumian, M., 2013. Relevance of Nanotechnology to Africa: Synthesis, Applications, and Safety, in: Gurib-Fakim, A., Eloff, J.N. (Eds.), Chemistry for Sustainable Development in Africa. Springer Berlin Heidelberg, Berlin, Heidelberg, pp. 123–158. https://doi.org/10.1007/978-3-642-29642-0_8.
4. Soares KSR, Formiga ALD, Uchôa AFC, Cardoso ALMR, Rodrigues JPCG, Leite JdePFB, Silva LFA, Alves ÁEF, Barbosa-Filho JM, Xavier-Junior FH (2025) Beyond the peril of envenomation: a nanotechnology approach for therapeutic venom delivery. J Drug Deliv Sci Technol 105:106652. https://doi.org/10.1016/j.jddst.2025.106652
5. Hsiao I-L, Huang Y-J (2011) Effects of various physicochemical characteristics on the toxicities of ZnO and TiO_2 nanoparticles toward human lung epithelial cells. Sci Total Environ 409:1219–1228
6. Oberdörster G, Oberdörster E, Oberdörster J (2005) Nanotoxicology: an emerging discipline evolving from studies of ultrafine particles. Environ Health Perspect 113:823–839. https://doi.org/10.1289/ehp.7339
7. Karlsson HL (2010) The comet assay in nanotoxicology research. Anal Bioanal Chem 398:651–666. https://doi.org/10.1007/s00216-010-3977-0
8. Saman S, Moradhaseli S, Shokouhian A, Ghorbani M (2013) Histopathological effects of ZnO nanoparticles on liver and heart tissues in Wistar rats. Adv Biores 4:83–88
9. Baranowska-Wójcik E, Szwajgier D, Oleszczuk P, Winiarska-Mieczan A (2020) Effects of titanium dioxide nanoparticles exposure on human health—a review. Biol Trace Elem Res 193:118–129. https://doi.org/10.1007/s12011-019-01706-6
10. Allen R (2016) The cytotoxic and genotoxic potential of titanium dioxide (TiO_2) nanoparticles on human SH-SY5Y neuronal cells in vitro. Plymouth Stud Sci 9:5–28
11. Dobrzyńska MM, Gajowik A, Radzikowska J, Lankoff A, Dušinská M, Kruszewski M (2014) Genotoxicity of silver and titanium dioxide nanoparticles in bone marrow cells of rats in vivo. Toxicology 315:86–91
12. Zhao J, Li N, Wang S, Zhao X, Wang J, Yan J, Ruan J, Wang H, Hong F (2010) The mechanism of oxidative damage in the nephrotoxicity of mice caused by nano-anatase TiO_2. J Exp Nanosci 5:447–462. https://doi.org/10.1080/17458081003628931
13. Chen J, Dong X, Zhao J, Tang G (2009) In vivo acute toxicity of titanium dioxide nanoparticles to mice after intraperitioneal injection. J Appl Toxicol 29:330–337. https://doi.org/10.1002/jat.1414
14. Duan Y, Liu J, Ma L, Li N, Liu H, Wang J, Zheng L, Liu C, Wang X, Zhao X (2010) Toxicological characteristics of nanoparticulate anatase titanium dioxide in mice. Biomaterials 31:894–899
15. Hosseini A, Razavi BM, Hosseinzadeh H (2023) Protective effects of pomegranate (*Punica granatum*) and its main components against natural and chemical toxic agents: a comprehensive review. Phytomedicine 109:154581. https://doi.org/10.1016/j.phymed.2022.154581
16. Bamidele FP, John AA, Bukoye OE, Hannah AO. A study of some effects of aqueous extract of neem (Azadirachta indica) leaves on the lead acetate

induced neurotoxicity in the superficial layers of superior colliculus of adult wistar rats (Rattus norvegicus)
17. Vasantharaj S, Sathiyavimal S, Hemashenpagam N (2013) Phytochemical analysis and antibacterial activity of *Azadirachta indica*. Int J Pharm Sci Rev Res 22:59–61
18. Newman DJ, Cragg GM (2016) Natural products as sources of new drugs from 1981 to 2014. J Nat Prod 79:629–661. https://doi.org/10.1021/acs.jnatprod.5b01055
19. Shukia R, Sharma SB, Puri D, Prabhu KM, Murthy PS (2000) Medicinal plants for treatment of diabetes mellitus. Indian J Clin Biochem 15:169–177. https://doi.org/10.1007/BF02867556
20. Fakunle PB, Samuel E, Roy A, Omotosho DA, Taiwo-Ola DO, Kayode O, Emmanuel CJ, Folahan OP (2024) Assessment of the ameliorative effects of aqueous neem (*Azadirachta Indica*) leaves extract on lead acetate induced neurotoxicity in cerebellum of adult Wistar rats. J Med Dental Sci Res 11:36–48
21. El-behairy DS, Diaa Eldin NH, Elbadry EE, Mohamed AA, Farrag IM (2019) Hepato-renal toxicity of titanium dioxide nanoparticles and the protective effects of *Moringa oleifera* leaves extract and vitamin E in male albino rats. Egypt J Hosp Med 75:2261–2271
22. Abu-Dief EE, Khalil KM, Abdel-Aziz HO, Nor-Eldin EK, Ragab EE (2015) Histological effects of titanium dioxide nanoparticles in adult male albino rat liver and possible prophylactic effects of milk thistle seeds. Life Sci J 12:115–123
23. Zhang H, Song W, Zheng L (2025) Pre-harvest low-dose UV-B irradiation improves the accumulation of bioactive component and post-harvest shelf-life of *Mesembryanthemum crystallinum*. J Agric Food Res 19:101737. https://doi.org/10.1016/j.jafr.2025.101737
24. Tuyen VTX, Khai TV, Diem NTT, Xuan LNT, Tan ND (2025) Effect of supplied salt concentrations in the nutrient solution during hydroponic production on phytochemicals and antioxidant activity of ice plants (*Mesembryanthemum crystallinum* L.). Int J Agric Biosci 14:59–67
25. Kang Y-W, Joo N-M (2023) Optimization of nutrient-rich ice plant (*Mesembryanthemum crystallinum* L.) paste fresh noodle pasta using response surface methodology. Foods 12:2482
26. Ibtissem B, Abdelly C, Sfar S (2012) Antioxidant and antibacterial properties of *Mesembryanthemum crystallinum* and *Carpobrotus edulis* extracts. Adv Chem Eng Sci 2:359–365
27. Nam S, Kang S, Kim S, Ko K (2017) Effect of fermented ice plant (*Mesembryanthemum crystallinum* L.) extracts against antioxidant, antidiabetic and liver protection. J Life Sci 27:909–918
28. Lee B-H, Lee C-C, Wu S-C (2014) Ice plant (*Mesembryanthemum crystallinum*) improves hyperglycaemia and memory impairments in a Wistar rat model of streptozotocin-induced diabetes: anti-diabetic neuropathy of ice plant. J Sci Food Agric 94:2266–2273. https://doi.org/10.1002/jsfa.6552
29. Burana C, Congtrakultien M, Kamthornsiriwimol N (2020) A novel growth and development of *Mesembryanthemum crystallinum* (Aizoaceae) in Thailand. Int Sci J Eng Technol ISJET 4:1–5
30. Alara OR, Abdurahman NH, Olalere OA (2020) Ethanolic extraction of flavonoids, phenolics and antioxidants from *Vernonia amygdalina* leaf using two-level factorial design. J King Saud Univ 32:7–16
31. Ribarova F, Atanassova M, Marinova D, Ribarova F, Atanassova M (2005) Total phenolics and flavonoids in Bulgarian fruits and vegetables. JU Chem Met 40:255–260
32. Broadhurst RB, Jones WT (1978) Analysis of condensed tannins using acidified vanillin. J Sci Food Agric 29:788–794. https://doi.org/10.1002/jsfa.2740290908
33. Le V, Parks AE, Nguyen SH, Roach MD (2018) Improving the vanillin-sulphuric acid method for quantifying total saponins. Technologies 6:84
34. Roberts R, Elias R. Determination of carbohydrate using phenol sulphuric acid method. Food analysis. 2011:234-7.
35. Prieto P, Pineda M, Aguilar M (1999) Spectrophotometric quantitation of antioxidant capacity through the formation of a phosphomolybdenum complex: specific application to the determination of vitamin E. Anal Biochem 269:337–341
36. Kavak C, Başẗürk A (2020) Antioxidant activity, volatile compounds and fatty acid compositions of *Cephalaria syriaca* seeds obtained from different regions in Turkey. Grasas Aceites 71:e379. https://doi.org/10.3989/gya.0913192
37. Riyadh M, S., M. Gomha, S., A. Mahmmoud, E., M. Elaasser, M., (2015) Synthesis and anticancer activities of thiazoles, 1,3-thiazines, and thiazolidine using chitosan-grafted-poly(vinylpyridine) as basic catalyst. Heterocycles 91:1227. https://doi.org/10.3987/COM-15-13210
38. El-Nekeety AA, Hassan ME, Hassan RR, Elshafey OI, Hamza ZK, Abdel-Aziem SH, Hassan NS, Abdel-Wahhab MA (2021) Nanoencapsulation of basil essential oil alleviates the oxidative stress, genotoxicity and DNA damage in rats exposed to BHE inflammatory process in responseiosynthesized iron nanoparticles. Heliyon 7:e07537. https://doi.org/10.1016/j.heliyon.2021.e07537
39. Adams, R.P., 2017. Identification of essential oil components by gas chromatography/mass spectrometry, 4.1. Allured Publ Crop Carol Steam IL.
40. Theivasanthi, T., Alagar, M., 2013. Titanium dioxide (TiO2) Nanoparticles XRD Analyses: An Insight. https://doi.org/10.48550/arXiv.1307.1091.
41. Orazizadeh M, Fakhredini F, Mansouri E, Khorsandi L (2014) Effect of glycyrrhizic acid on titanium dioxide nanoparticles-induced hepatotoxicity in rats. Chem Biol Interact 220:214–221
42. Lin R-Y, Vera JC, Chaganti RS, Golde DW (1998) Human monocarboxylate transporter 2 (MCT2) is a high affinity pyruvate transporter. J Biol Chem 273:28959–28965
43. Hill CP, Worthylake D, Bancroft DP, Christensen AM, Sundquist WI (1996) Crystal structures of the trimeric human immunodeficiency virus type 1 matrix protein: implications for membrane association and assembly. Proc Natl Acad Sci USA 93:3099–3104. https://doi.org/10.1073/pnas.93.7.3099
44. Bancroft JD, Gamble M (2008) Theory and practice of histological techniques. Elsevier health sciences.
45. Braga RC, Alves VM, Muratov EN, Strickland J, Kleinstreuer N, Trospsha A, Andrade CH (2017) Pred-skin: a fast and reliable web application to assess skin sensitization effect of chemicals. J Chem Inf Model 57:1013–1017. https://doi.org/10.1021/acs.jcim.7b00194
46. Banerjee P, Eckert AO, Schrey AK, Preissner R (2018) ProTox-II: a webserver for the prediction of toxicity of chemicals. Nucleic Acids Res 46:W257–W263
47. Duy, T.N., Tuyet, L.V.T., Van, K.T., Xuan, T.V.T., 2025. Analysis of nutritional and antioxidant components of ice plant grown in An Giang, Vietnam. Plant Sci Today https://doi.org/10.14719/pst.3944.
48. Abuajah CI, Ogbonna AC, Osuji CM (2015) Functional components and medicinal properties of food: a review. J Food Sci Technol 52:2522–2529
49. Boik J (2001) Natural compounds in cancer therapy.
50. Lauson CBN, Tiberti S, Corsetto PA, Conte F, Tyagi P, Machwirth M, Ebert S, Loffreda A, Scheller L, Sheta D (2023) Linoleic acid potentiates CD8+ T cell metabolic fitness and antitumor immunity. Cell Metab 35:633–650
51. Anandakumar P, Vanitha MK, Gizaw M, Dereje G (2018) A review on the diverse effects of D-pinitol. Adv J Pharm Life Sci Res 6:1–7
52. Sadat SM, Jahan ST, Haddadi A (2016) Effects of size and surface charge of polymeric nanoparticles on in vitro and in vivo applications. J Biomater Nanobiotechnology 7:91
53. Ramakrishnan M, Shanmugam R, Neeharika S, Chokkattu JJ, Thangavelu L, Khanna N (2023) Anti-inflammatory activity and cytotoxic effect of ginger and rosemary-mediated titanium oxide nanoparticles-based dental varnish. World J Dent 14:761–765. https://doi.org/10.5005/jp-journals-10015-229
54. Maanane F, El Yadini A, El Alouani M, Mabrouki J, Saufi H, Tabyaoui M (2023) Green development of titanium dioxide using *Astragalus boeticus* for the degradation of cationic and anionic dyes in an aqueous environment. Water 15:3471
55. Hong F, Wu N, Zhao X, Tian Y, Zhou Y, Chen T, Zhai Y, Ji L (2016) Titanium dioxide nanoparticle-induced dysfunction of cardiac hemodynamics is involved in cardiac inflammation in mice: nanoparticle-induced dysfunction of cardiac hemodynamics. J Biomed Mater Res A 104:2917–2927
56. McClements D, Julian L, Chengmei Z, Liqiang X. Encapsulation of protein nanoparticles within alginate microparticles: Impact of pH and ionic strength on 2 functional performance 3. J. Food Eng.. 2016:178.
57. Akagi J, Mizuta Y, Akane H, Toyoda T, Ogawa K (2023) Oral toxicological study of titanium dioxide nanoparticles with a crystallite diameter of 6 nm in rats. Part Fibre Toxicol 20:23. https://doi.org/10.1186/s12989-023-00533-x
58. Wani MR, Maheshwari N, Shadab G (2021) Eugenol attenuates TiO_2 nanoparticles-induced oxidative damage, biochemical toxicity and DNA

damage in Wistar rats: an in vivo study. Environ Sci Pollut Res 28:22664–22678. https://doi.org/10.1007/s11356-020-12139-3
59. Thapa BR, Walia A (2007) Liver function tests and their interpretation. Indian J Pediatr 74:663–671. https://doi.org/10.1007/s12098-007-0118-7
60. Abdel-Wahhab MA, El-Nekeety AA, Mohammed HE, Elshafey OI, Abdel-Aziem SH, Hassan NS (2021) Elimination of oxidative stress and genotoxicity of biosynthesized titanium dioxide nanoparticles in rats via supplementation with whey protein-coated thyme essential oil. Environ Sci Pollut Res 28:57640–57656. https://doi.org/10.1007/s11356-021-14723-7
61. Reeves JF, Davies SJ, Dodd NJ, Jha AN (2008) Hydroxyl radicals (OH) are associated with titanium dioxide (TiO_2) nanoparticle-induced cytotoxicity and oxidative DNA damage in fish cells. Mutation Res Fundament Mol Mech Mutagenesis 640:113–122
62. Rajapakse K, Drobne D, Valant J, Vodovnik M, Levart A, Marinsek-Logar R (2012) Acclimation of *Tetrahymena thermophila* to bulk and nano-TiO2 particles by changes in membrane fatty acids saturation. J Hazard Mater 221:199–205
63. Trouiller B, Reliene R, Westbrook A, Solaimani P, Schiestl RH (2009) Titanium dioxide nanoparticles induce DNA damage and genetic instability in vivo in mice. Cancer Res 69:8784–8789
64. Shi Y, Jiang J, Shan Z, Bu Y, Deng Z, Cheng Y (2015) Oxidative stress and histopathological alterations in liver of *Cyprinus carpio* L. induced by intraperitoneal injection of microcystin-LR. Ecotoxicology 24:511–519. https://doi.org/10.1007/s10646-014-1399-z
65. Sharma N (2014) Free radicals, antioxidants and disease. Biol Med 6:1
66. Albrahim T, Alonazi MA (2020) Role of beetroot (*Beta vulgaris*) juice on chronic nanotoxicity of silver nanoparticle-induced hepatotoxicity in male rats. Int J Nanomedicine 15:3471–3482. https://doi.org/10.2147/IJN.S248078
67. Jani PU, McCarthy DE, Florence AT (1994) Titanium dioxide (rutile) particle uptake from the rat GI tract and translocation to systemic organs after oral administration. Int J Pharm 105:157–168
68. Wang J, Zhou G, Chen C, Yu H, Wang T, Ma Y, Jia G, Gao Y, Li B, Sun J (2007) Acute toxicity and biodistribution of different sized titanium dioxide particles in mice after oral administration. Toxicol Lett 168:176–185
69. Huggins CB, Froehlich JP (1966) High concentration of injected titanium dioxide in abdominal lymph nodes. J Exp Med 124:1099
70. Ajit P, Rahul S, Suyash S (2024) Cytopathology: an important aspect of medical diagnosis. Res Rev J Oncol Hematol 12:13–18
71. Valentini F, Kozell V, Petrucci C, Marrocchi A, Gu Y, Gelman D, Vaccaro L (2019) Formic acid, a biomass-derived source of energy and hydrogen for biomass upgrading. Energy Environ Sci 12:2646–2664
72. Olmedo DG, Tasat DR, Evelson P, Guglielmotti MB, Cabrini RL (2008) Biological response of tissues with macrophagic activity to titanium dioxide. J Biomed Mater Res A 84A:1087–1093. https://doi.org/10.1002/jbm.a.31514
73. Epstein MS, Blackburn DG (1997) Histology and histochemistry of androgen-stimulated nuptial pads in the leopard frog, *Rana pipiens*, with notes on nuptial gland evolution. Can J Zool 75:472–477. https://doi.org/10.1139/z97-057
74. Behairy A, Hashem MM, Abo-EL-Sooud K, Soliman AM, Mouneir SM, El-Metwally AE, Ismail SH, Hassan BA, Abd-Elhakim YM (2024) Influence of titanium dioxide nanoparticles and/or cadmium chloride oral exposure on testicular morphology, oxidative stress, and apoptosis in rats: ameliorative role of co-enzyme Q10. Heliyon. https://doi.org/10.1016/j.heliyon.2024.e24049
75. Ślesak I, Miszalski Z, Karpinska B, Niewiadomska E, Ratajczak R, Karpinski S (2002) Redox control of oxidative stress responses in the C3–CAM intermediate plant *Mesembryanthemum crystallinum*. Plant Physiol Biochem 40:669–677
76. Drira R, Matsumoto T, Agawa M, Sakamoto K (2016) Ice plant (*Mesembryanthemum crystallinum*) extract promotes lipolysis in mouse 3T3-L1 adipocytes through extracellular signal-regulated kinase activation. J Med Food 19:274–280. https://doi.org/10.1089/jmf.2015.3470
77. Khemakhem B, El Abed H, Chakroun M, Fendri I, Smaoui S (2019) Functional effects of ice plant amylases on cake and bun quality. Food Biosci 29:142–149
78. Calvo MM, Martín-Diana AB, Rico D, López-Caballero ME, Martínez-Álvarez O (2022) Antioxidant, antihypertensive, hypoglycaemic and nootropic activity of a polyphenolic extract from the halophyte Ice Plant (*Mesembryanthemum crystallinum*). Foods 11:1581
79. Shabbir S, Kulyar MF-A, Bhutta ZA, Boruah P, Asif M (2021) Toxicological consequences of titanium dioxide nanoparticles (TiO2NPs) and their jeopardy to human population. BioNanoScience 11:621–632. https://doi.org/10.1007/s12668-021-00836-3
80. Jabeen, S., Noor, S., 2024. Oxidative stress and chronic kidney disease, in: fundamental principles of oxidative stress in metabolism and reproduction. Elsevier, pp. 151–165.
81. Ma Z-G, Yuan Y-P, Xu S-C, Wei W-Y, Xu C-R, Zhang X, Wu Q-Q, Liao H-H, Ni J, Tang Q-Z (2017) CTRP3 attenuates cardiac dysfunction, inflammation, oxidative stress and cell death in diabetic cardiomyopathy in rats. Diabetologia 60:1126–1137. https://doi.org/10.1007/s00125-017-4232-4
82. Elvira-Torales LI, García-Alonso J, Periago-Castón MJ (2019) Nutritional importance of carotenoids and their effect on liver health: a review. Antioxidants 8:229
83. Aleebrahim-Dehkordy E, Khodadadi S, Mousavipanah Z, Nasri H (2016) Herbal antioxidants and kidney. Ann Res Antioxid 1:e10
84. Pisoschi AM, Pop A, Iordache F, Stanca L, Predoi G, Serban AI (2021) Oxidative stress mitigation by antioxidants-an overview on their chemistry and influences on health status. Eur J Med Chem 209:112891
85. Hajirezaee S, Mohammadi G, Naserabad SS (2020) The protective effects of vitamin C on common carp (*Cyprinus carpio*) exposed to titanium oxide nanoparticles (TiO_2-NPs). Aquaculture 518:734734
86. Kong L, Hu W, Lu C, Cheng K, Tang M (2019) Mechanisms underlying nickel nanoparticle induced reproductive toxicity and chemo-protective effects of vitamin C in male rats. Chemosphere 218:259–265
87. Abdelhalim M, Moussa S, Qaid H (2018) The protective role of quercetin and arginine on gold nanoparticles induced hepatotoxicity in rats. Int J Nanomedicine 13:2821–2825. https://doi.org/10.2147/IJN.S160995
88. de Carvalho APA, Conte-Junior CA (2021) Health benefits of phytochemicals from Brazilian native foods and plants: antioxidant, antimicrobial, anti-cancer, and risk factors of metabolic/endocrine disorders control. Trends Food Sci Technol 111:534–548
89. Hamed HS, Abdel-Tawwab M (2021) Dietary pomegranate (*Punica granatum*) peel mitigated the adverse effects of silver nanoparticles on the performance, haemato-biochemical, antioxidant, and immune responses of Nile tilapia fingerlings. Aquaculture 540:736742
90. Rowida YE, Elsebaie E (2018) Ice plant as antioxidant/anticancer and functional food. World J Dairy Food Sci 13:57–62
91. Lee D, Kim SJ, Choi YJ, Rho YH, Kang TS, Kim YG, Kang KS (2025) The glucose-lowering effect of *Mesembryanthemum crystallinum* and D-pinitol: studies on insulin secretion in INS-1 cells and the reduction of blood glucose in diabetic rats. Nutrients 17:193

Publisher's Note

Springer Nature remains neutral with regard to jurisdictional claims in published maps and institutional affiliations.